공학석사학위논문

The Effect of Composition on Microstructure and Mechanical Properties of Extruded Magnesium ZAxy Alloy

2012 년 12 월

서울대학교 대학원

재료공학부

Jiang Hansi

The Effect of Composition on Microstructure and Mechanical Properties of Extruded Magnesium ZAxy Alloy

지도교수 신 광 선

이 논문을 공학 석사학위 논문으로 제출함

2012 년 12 월

서울대학교 대학원

재료공학부

Jiang Hansi

Jiang Hansi 의 공학석사 학위논문을 인준함

2012 년 12 월

위 원 장 한 홍 남 (인)

부위원장 신 광 선 (인)

위 원 박 은 수 (인)

Abstract

The Effect of Composition on Microstructure and Mechanical Properties of Extruded Magnesium ZAxy Alloy

Jiang Hansi

School of Material Science and Engineering

The Graduate School

Seoul National University

Limited formability at low temperature of wrought magnesium alloys which is caused by the hexagonal close packed crystal structure and the strong basal texture limits the applications in lightweight structure parts. In order to improve the poor ductility and the anisotropic mechanical properties of Mg alloys, new Mg-Zn based wrought Mg alloys were developed. Billets of Mg-Zn-Al alloys with different compositions were fabricated by gravity casting followed by homogenization treatment and extruded. The microstructures were observed by the optical microscopy (OM). The effects of Zn and Al on deformation behavior were examined by tensile and compressive tests. The changes of texture by plastic deformation were tested using the X-ray diffraction machine. The basal poles (002) spread along the extrusion (Rolling) direction.

Key words: Mg-Zn-Al alloy; Extrusion; Microstructure; Mechanical Property; Texture

Student Number: 2010-24050

Contents

List of Tables

List of Figures

1. INTRODUCTION

1.1 Magnesium Alloys

Magnesium alloys are the lightest structural metallic materials with excellent properties such as high specific strength, superior damping characteristics, good mold ability and electromagnetic shielding performance so they are paid great attention intensively as “the green project materials having development potential and best future in the 21st century” [1-2].

The use of magnesium and magnesium alloys as a structural material is growing. This growth is being driven primarily by the automotive industry. Growth of magnesium use in the automotive industry has been estimated at 15% each year over the past decade. This growth is expected to continue at an annual rate of 12% over the next decade [3]. Demands for increased fuel efficiency in automobiles and cost effective manufacturing of parts have created this growth. Consumers’ demands for increased luxury and safety features have caused an increase in vehicle weight translating into increased fuel consumption and ultimately increased CO2 emissions. It is well known that CO2 is a potent greenhouse gas. Magnesium has one major advantage over other structural materials, low density. With a density that is approximately two-thirds that of aluminum, the potential weight savings due to increased magnesium use has substantial environmental impact, including reduction of greenhouse gas emissions. Furthermore global environmental policy requires reusability and recyclability, and magnesium, unlike many polymers is a recyclable material. Although magnesium alloys have been developed and used for the better part of the last century, research and development of magnesium alloys significantly declined after the 1960’s as a result of an unfavorable price differential between magnesium and aluminum, and magnesium alloys were no longer needed to support war activities as a material in ballistic ordinance and aircraft. As a result, the metallurgical knowledge of magnesium and its

alloys is immature compared to that of aluminum and its alloys leaving a significant amount of work waiting for the attention of researchers.

Because magnesium has HCP crystal structure with little slip system, plastic deformation is hard at room temperature [4]. At the same time, magnesium alloy castings exist many defects, such as unsound microstructure, low material utilization and reliability. Consequently its application is still limited to a narrow field. For conventional magnesium alloys, the strength and the elongation are not so high [5-6], which limits its application for structural use. Hot-forging, hot-extruding and hot-rolling are the efficiency ways to improve the formability of the magnesium alloys. Magnesium alloys produced by these methods can extend application range due to higher strength, better plasticity and various mechanical properties. Therefore, amelio rating the process and improving the mechanical properties of wrought magnesium alloys are of great scientific significance [7].

1.2 Mg-Zn-Al alloys and application

Die casting is one of the most effective fabrication methods and has been extensively used to produce magnesium components, especially in the automotive industry. However, the number of available Mg-based alloys for die casting is very limited. At the present time, AZ91 is still the most commonly used die casting alloy. Although AZ91 offers a good combination of mechanical properties, corrosion resistance and die castability, it is unsuitable for use at temperatures above 120°C due to its poor creep resistance and its decrease in strength at elevated temperatures. [8-11]. Therefore, it is pressing to develop some new Mg die casting alloys with good creep resistance, acceptable castability and low cost.

Figure 1.2.1 shows the Mg-Zn-Al ternary phase diagram. The thermal signals at low temperature shown in Figure 1.2.2 are associated with phase equilibria involving

more than two solid phases. Phase equilibria of the Mg–Al–Mn–Zn quaternary system provide crucial information in development and designing of Mg-alloys like the significant AZ and AM series. The main goal of the series of present studies is to establish the thermodynamic description for the Mg–Al–Mn–Zn system on the basis of well assessed and properly interpreted experimental data. To this end, the thermodynamic description for each sub-ternary system as well as sub-binary system needs to be obtained, scrutinized or improved to compute the phase equilibria with high precision [12].

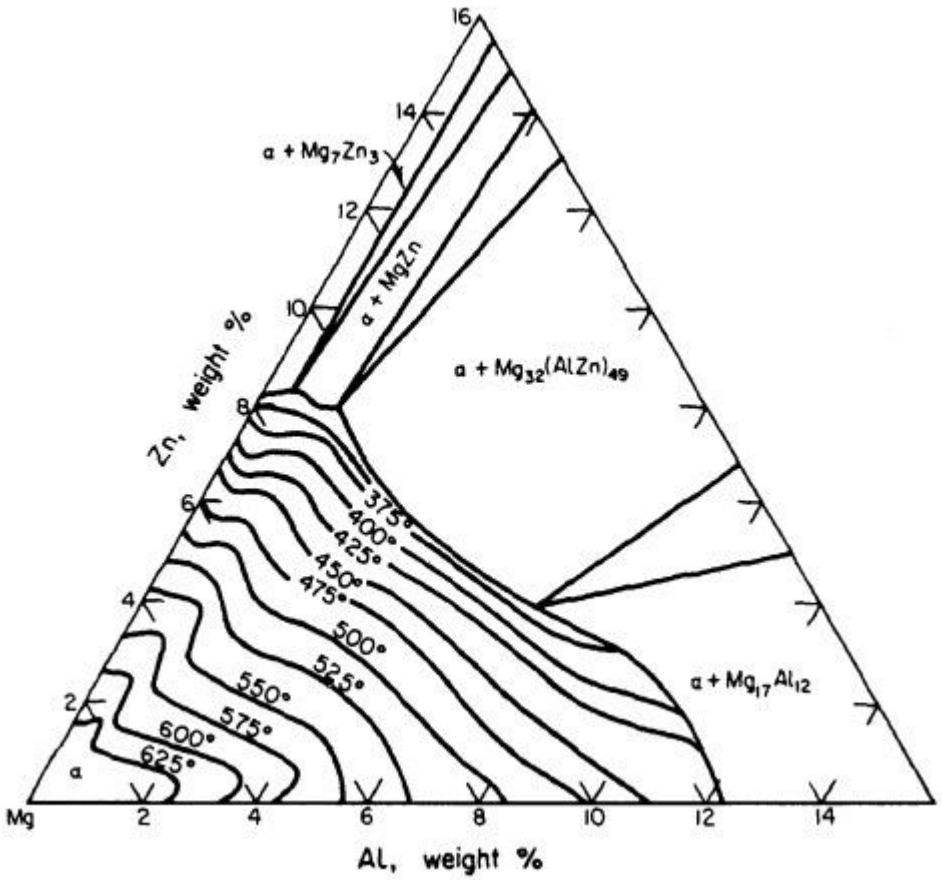

Figure 1.2.1 Mg-Zn-Al ternary phase diagram (solidus surface). [13]

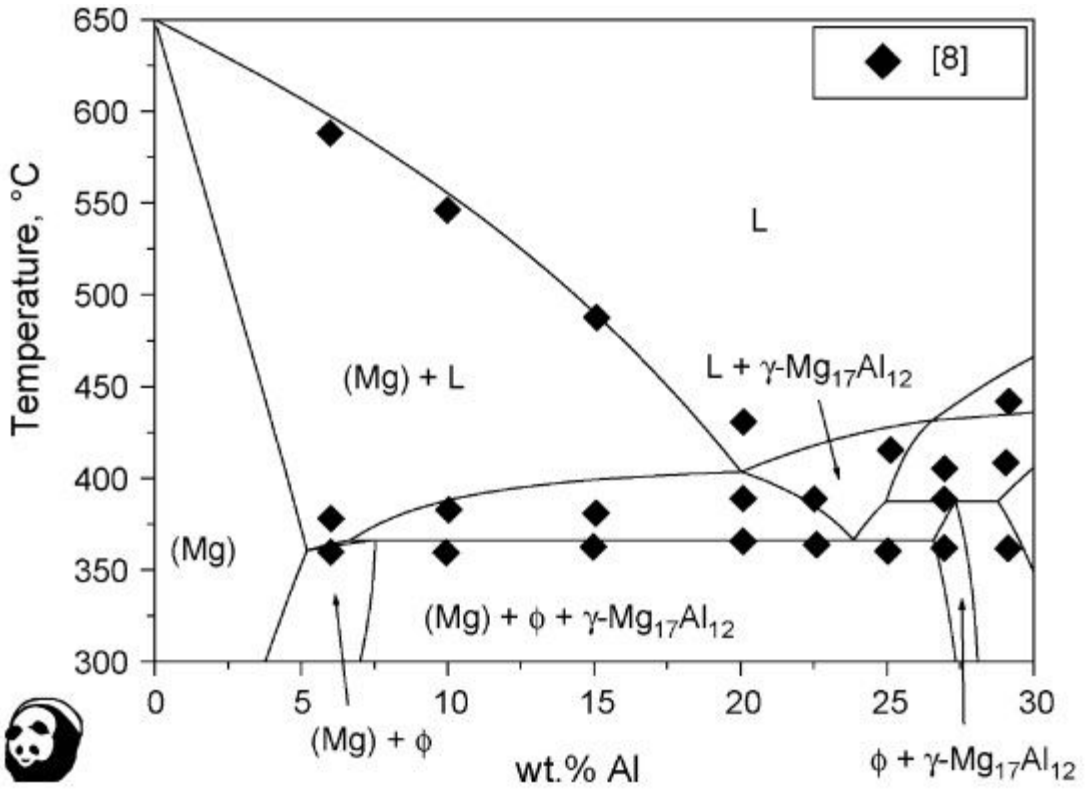

Figure 1.2.2 The Mg–Al–Zn(Al:Zn-1:1) phase diagram at fixed compositions with the experimental data of thermal analysis.

As expected from the phase diagram (Figure Mg-Al phase diagram), Mg-Al alloys are precipitation heat treatable, although solutionizing and aging of Mg-Al alloys do not have the effectiveness seen in many Al-Si alloys as the ß- Mg17Al12 precipitate forms in an incoherent manner [14-15].

Mg-Al binary alloys are generally highly castable and typically have good mechanical properties. However, commercial alloys are rarely binary alloys; they are mostly ternary and quaternary alloys with additions of zinc, manganese, rare earth metals, and silicon. These additions improve specific properties as was discussed earlier and make the alloys more suitable for casting; however, they also complicate the solidification behavior of the alloy [16-17].

Mg-Al-Zn alloys are the most widely used wrought alloys at present because of their abundant raw materials and low price. Wrought materials are produced mainly be extrusion, rolling and press forging at temperatures in the range 300-500℃ with cast billet for products of transportation such as aircraft, automobile and so on. Generally, wrought magnesium alloys are Mg-Zn, Mg-Zn-Al, Mg-Zn-Zr, Mg-Zn-RE, Mg-Th alloy and so on.

Mg alloys application---Focusing on automobile applications (Figure 1.2.3), magnesium flat rolled products offer potential for nearly all car areas. Besides a significant reduction of weight and improved weight distribution in terms of a lighter front area, the lowering of the point of gravity and the reduction of unsprung masses should lead to better driving performance. Fields of application include the interior (e.g., bracket car- rier, seat components); the body (large hang-on parts like doors, roof, bonnets, as well as body in white and front end parts); the drive system (cylinder head cover, oil pan), as well as the chassis (e.g., wheels).

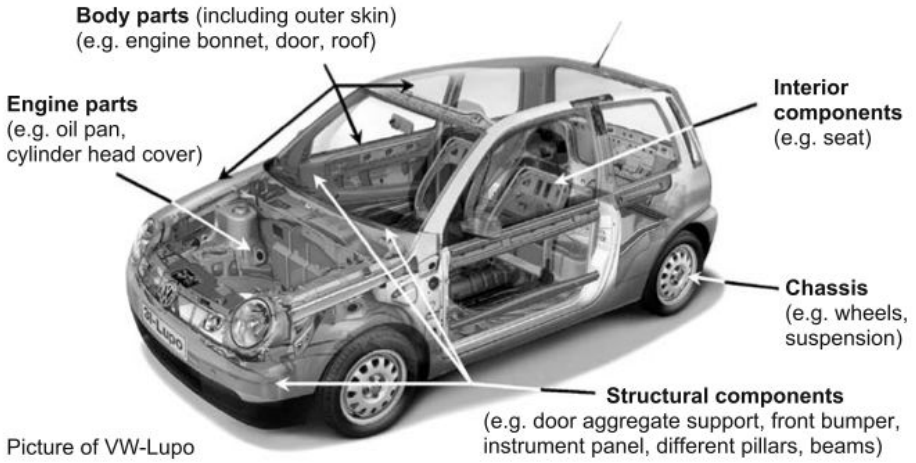

Figure 1.2.3 Magnesium alloys of automobile applications.

1.3 Solidification Behavior of Magnesium Alloys

The final microstructure of Mg-Al (1.3.1) alloys will be dependent on the nucleation and growth characteristics, of both the primary grains and the eutectic [16]. Therefore, alloying elements, grain refiners, and cooling rate during solidification will all have a major effect on the final microstructure and properties of the cast alloy. Nucleation is typically controlled by the use of grain refiners. Grain refinement in magnesium casting alloys is not as well understood as in aluminum casting alloys [16]. The growth morphologies of both the primary dendrites and the eutectic in the Mg-Al system are highly dependant on the aluminum content and cooling rate [16].

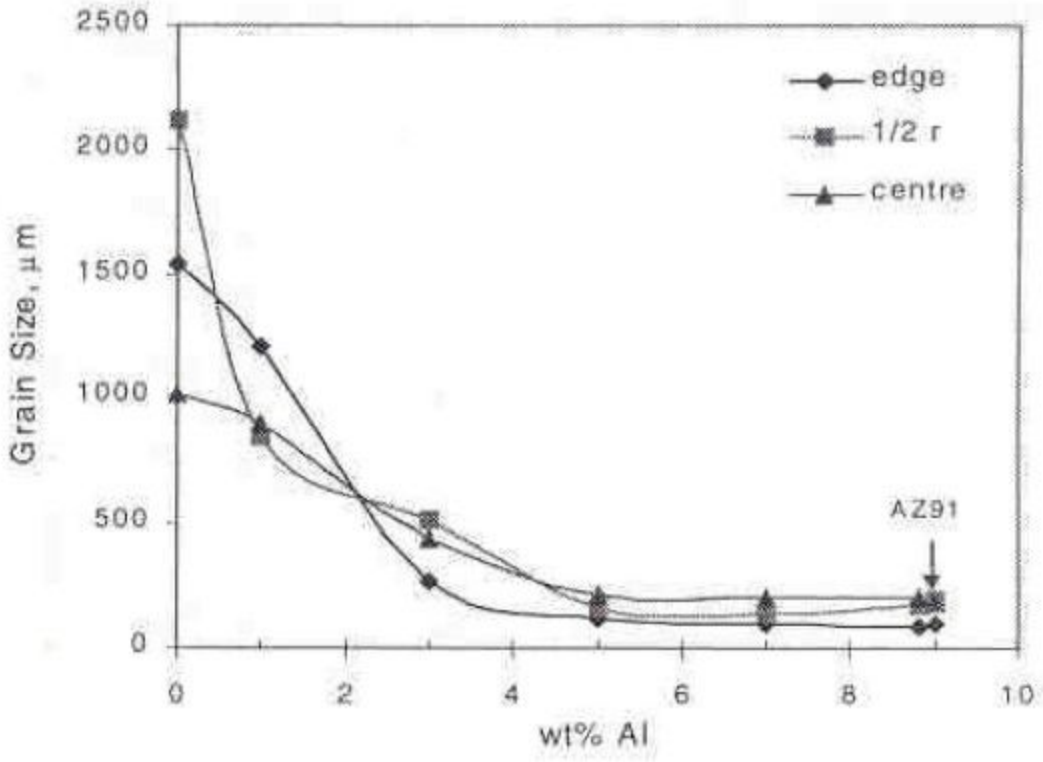

Figure 1.3.1 Grain Refining Effects of Al in Pure Mg. [30]

A reliable grain refiner for the Mg-Al system is lacking. Zirconium has been found to be a satisfactory grain refiner for some magnesium alloys, but Zr is not used in the alumi num containing alloys. Nevertheless, most Mg-Al alloys are used for high pressure die-casting, and this process has very high cooling rates, which introduces a high driving force for nucleation. This causes increased nucleation and therefore creates a large number of primary grains thus reducing the need for a potent grain refiner. Alloys based on the Mg-Zn and the Mg-RE (rare earth addition) have been found to form very fine grains when Zr is added. The mechanism of Zr grain refinement is poorly understood, but is believed to be caused by the crystal structure and lattice parameter similarity of Mg and Zr [16].

Recent research has been done in order to determine a better method of grain refining aluminum based magnesium alloys. Work by Lee et al [16] has shown the effects of aluminum and strontium (Sr) additions on grain size of magnesium alloys. It was found that grain size decreases dramatically when increasing the Al content of the alloy from 0wt% to 5wt%, but further additions have no effect. Figure 2 shows the grain refining effects of Al in pure Mg. Lee et al al [16] also investigated the effects of Sr addition on Mg-Al alloys for both Mg- 3wt%Al and Mg-9wt%Al alloys. The results show that a 0.01-0.1wt%Sr addition has a very strong grain refining effect on the 3wt%Al alloys as it decreases the average grain size by about 100 μm. The results for the 9wt%Al alloy show a narrower range of grain refining effect and in most cases no difference was observed.

1.4 Dynamic recrystallization

The softening processes of recovery and recrystallization may occur during deformation at high temperature, in this case the phenomena are called dynamic recovery and dynamic recrystallization (DRX) in order to distinguish them from the static annealing processes which occur during post deformation heat treatment. Figure

1.4.1 shows that schematic representation of possible softening process during hot-working [18]. The static and dynamic processes have many features in common, although the simultaneous operation of deformation and softening mechanisms leads to some important differences. Although dynamic restoration processes are of great industrial significance, they are not well under stood because they are difficult to study experimentally and to model theoretically. Dynamic recovery and DRX occur during metal working operations such as hot rolling, extrusion and forging. They are important because they lower the flow stress of material, thus enabling it to be deformed more easily and they also have an influence on the texture and the grain size of the worked material [19].

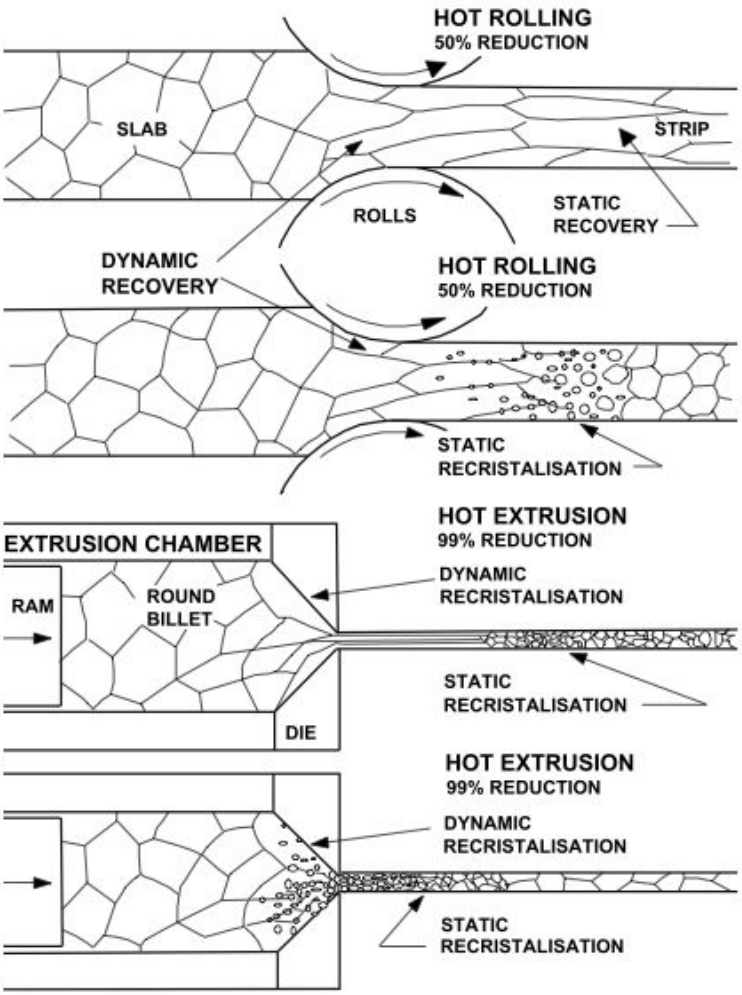

Figure 1.4.1 Schematic representation of possible softening process during hot-working.

1.5 Research objective

As expected from the phase diagram, Mg-Al alloys are precipitation heat treatable, although solutionizing and aging of Mg-Al alloys do not have the effectiveness seen in many Al-Si alloys as the ß- Mg17Al12 precipitate forms in an incoherent manner [14-15].

Mg-Al binary alloys are generally highly castable and typically have good mechanical properties. However, commercial alloys are rarely binary alloys; they are mostly ternary and quaternary alloys with additions of zinc, manganese, rare earth metals, and silicon. These additions improve specific properties as was discussed earlier and make the alloys more suitable for casting; however, they also complicate the solidification behavior of the alloy [16].

For achieving the development target of next generation automobiles, application fields of Mg alloy have to be expanded through not only development of cast alloy but also wrought magnesium alloy wich have high strength, toughness and formability and also new processes for manufacturing wrought magnesium alloys. The products of wrought magnesium alloy can also acquire higher high strength and toughness than cast magnesium alloy. Because of these, many works for controlling the microstructure, mechanical behavior and texture of wrought magnesium alloys by hot working process such as ECAP and DSR and also alloy development have been conducted. [20-25]

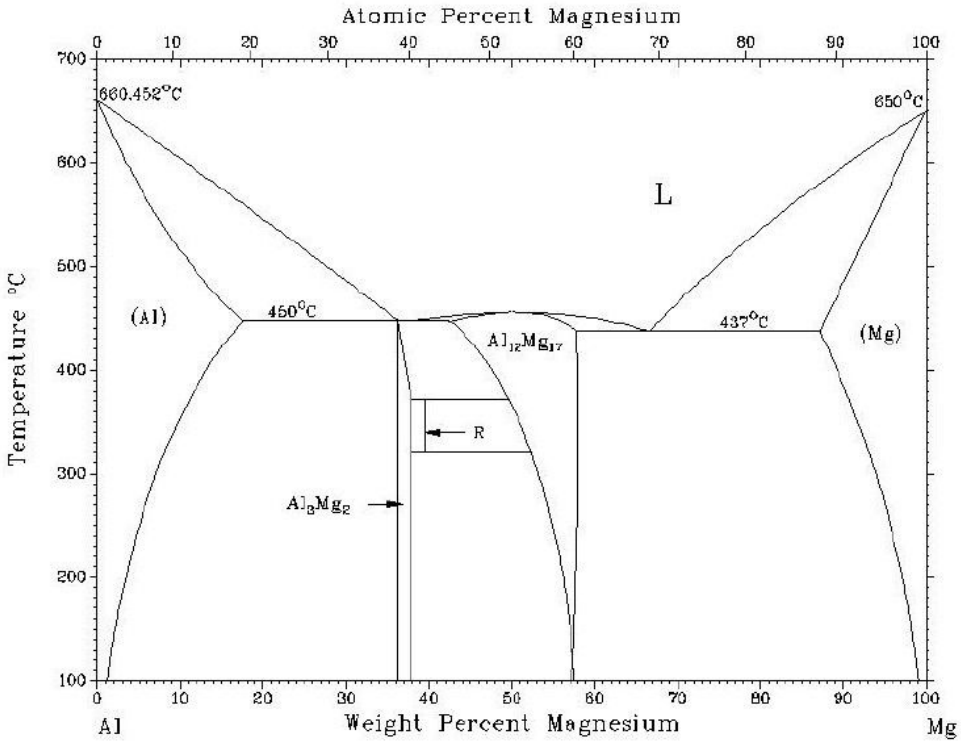

Figure 1.5.1 Mg-Al Phase Diagram [27].

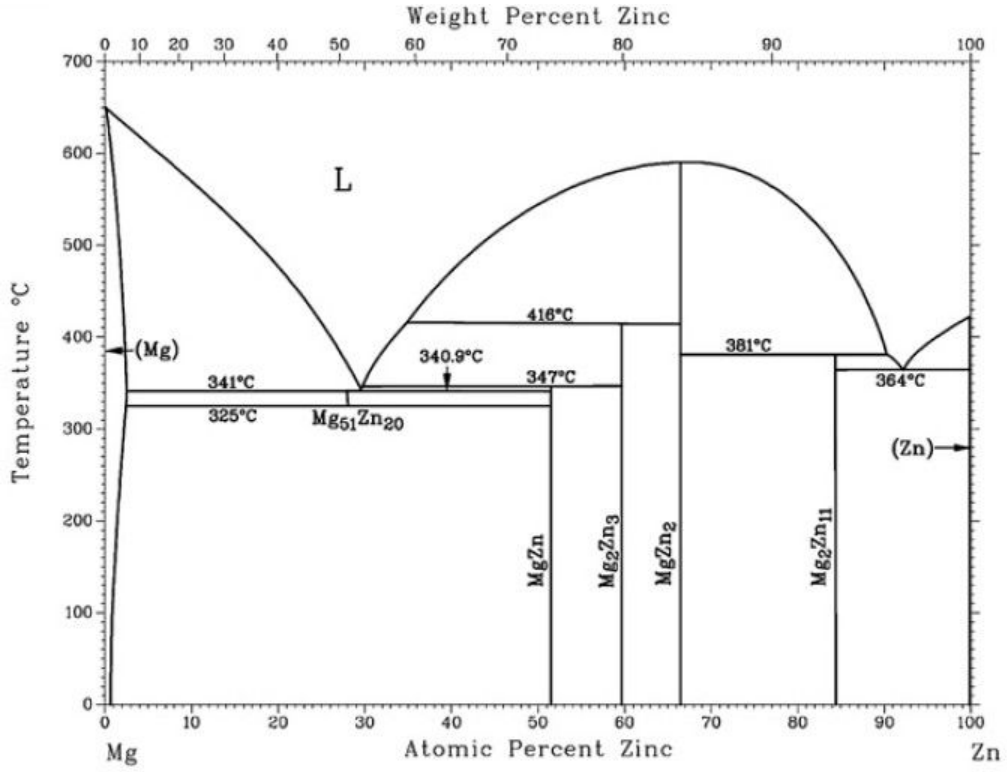

Figure 1.5.2 Phase diagram of MgZn [28].

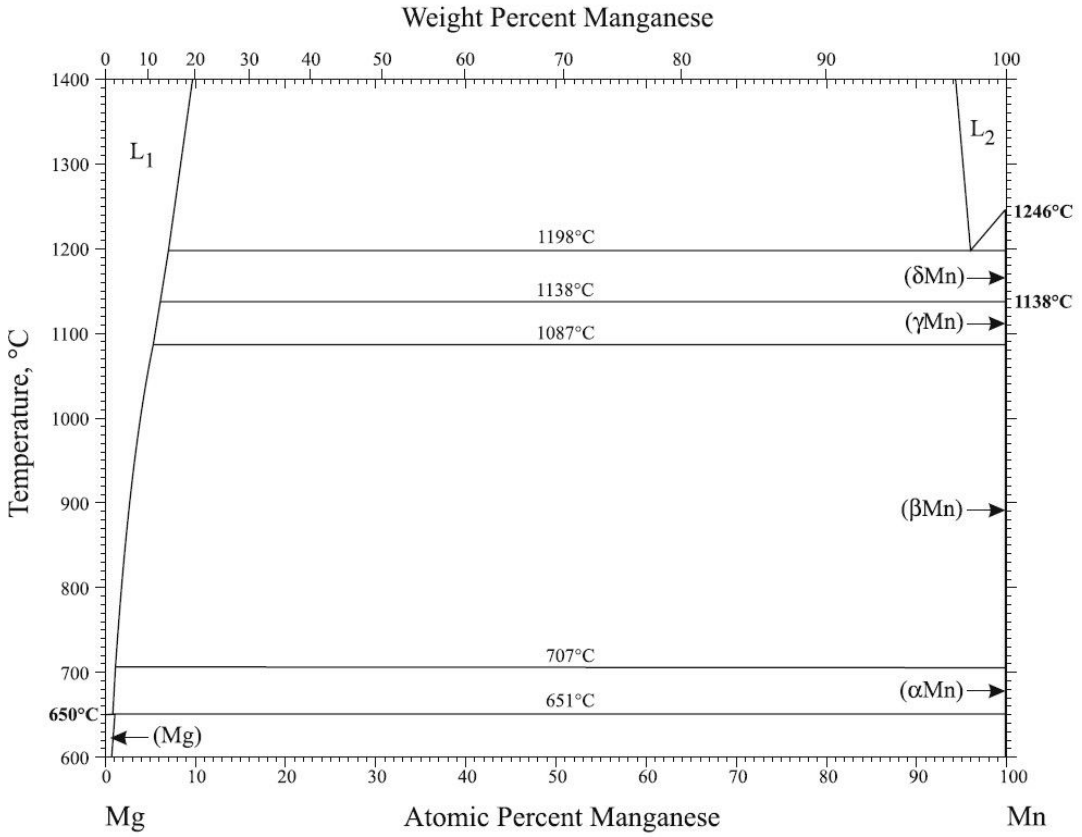

Figure 1.5.3 Mg-Mn phase diagram [29]

2. EXPERIMENTAL PROCEDURE

2.1 Fabrication of extruded ZA alloys

Chemical compositions of the billets of Mg-Zn-Al (ZAxy, in wt.%) are listed in Table 2.1.1. Alloy ingots are melted in a low-carbon steel crucible using resistance furnace(Figure 2.1.1) on 710℃ with stirring time Mn for 15min, Al for 5min and Zn for 5minto assure the homogeneity under the protection of mixed gas of 0.5%SF_6 and CO_2. The billets are homogenized at 300℃ for 12 hours under a gas of CO_2.

Alloy	Chemical Compositions (wt.%)			
	Zn	Al	Mn	Mg
ZA41	3.9	0.89	0.45	Bal.
ZA42	3.93	1.89	0.23	Bal.
ZA43	3.97	3.62	0.20	Bal.
ZA44	4.21	3.88	0.46	Bal.
ZA45	4.11	4.92	0.52	Bal.
ZA46	3.80	6.12	0.25	Bal.
ZA47	4.31	7.34	0.17	Bal.
ZA48	4.34	7.89	0.39	Bal.
ZA51	5.11	0.93	0.13	Bal.
ZA52	5.32	1.87	0.21	Bal.
ZA53	4.78	3.55	0.13	Bal.
ZA54	4.82	4.21	0.42	Bal.
ZA55	5.45	5.32	0.18	Bal.
ZA56	5.21	6.43	0.46	Bal.
ZA57	5.36	7.51	0.24	Bal.
ZA58	5.4	8.24	0.20	Bal.
ZA61	6.11	1.11	0.36	Bal.
ZA62	6.02	2.03	0.23	Bal.
ZA63	6.43	3.27	0.38	Bal.
ZA64	6.64	4.60	0.41	Bal.

Alloy	Chemical Compositions (wt.%)			
	Zn	Al	Mn	Mg
ZA65	6.30	5.48	0.12	Bal.
ZA66	6.31	6.20	0.23	Bal.
ZA67	5.73	6.72	0.21	Bal.
ZA68	5.81	8.21	0.41	Bal.
ZA71	6.69	0.73	0.26	Bal.
ZA72	6.86	2.41	0.36	Bal.
ZA73	6.81	2.79	0.17	Bal.
ZA74	7.42	4.21	0.23	Bal.
ZA75	7.31	4.85	0.42	Bal.
ZA76	7.24	6.23	0.27	Bal.
ZA77	7.45	6.89	0.12	Bal.
ZA78	7.21	8.34	0.22	Bal.
ZA81	8.32	1.15	0.12	Bal.
ZA82	8.25	2.04	0.46	Bal.
ZA83	7.89	3.23	0.21	Bal.
ZA84	7.69	4.34	0.25	Bal.
ZA85	8.14	4.78	0.51	Bal.
ZA86	7.82	5.87	0.11	Bal.
ZA87	7.91	7.14	0.19	Bal.
ZA88	8.43	7.90	0.21	Bal.

Table 2.1 Chemical compositions of magnesium alloys

Figure 2.1.1 Electronic Resistance Furnace

2.2Extrude the samples

The extrusion billets of are machined out from the homogenized billets. Before extrusion, the extrusion billets are pre-heated at 360℃ for 2 hours and the extrusion mould of 3mm×30mm plate type is pre-heated at 360℃ for 1 hour. The extrusion machine is shown in the figure 2.2.1 The extrusion condition is 340℃ with a speed of about 11 cm/min and the extrusion ratio is 56. The extrusion condition details are shown in Table2.2.

Figure 2.2.1 The extrusion machine.

	Billet Composition	Extruion Pressure (kg/cm^2)		Extrusion Speed (cm/min.)	Sample Length (m)
		Initial	Final		
1	ZA41	85	103	~13	3.2
2	ZA42	83	113	~15	3.1
3	ZA43	85	105	~11	3.1
4	ZA44	88	106	~11	3.2
5	ZA45	90	105	~10	3.2
6	ZA46	85	115	~12	3.3
7	ZA47	80	125	~14	3.4
8	ZA48	75	135	~16	3.3
9	ZA51	87	112	~14	3.0
10	ZA52	90	120	~14	3.2
11	ZA53	90	116	~11	3.1
12	ZA54	88	115	~12	3.2
13	ZA55	85	105	~11	3.1
14	ZA56	79	112	~14	3.2
15	ZA57	85	105	~12	3.1
16	ZA58	78	103	~11	3.2
17	ZA61	85	115	~15	3.1
18	ZA62	82	115	~13	3.2
19	ZA63	85	112	~16	3.2
20	ZA64	85	105	~14	3.1

	Billet Composition	Extruion Pressure (kg/cm^2)		Extrusion Speed (cm/min.)	Sample Length (m)
		Initial	Final		
21	ZA65	90	105	~14	3.2
22	ZA66	90	105	~13	3.2
23	ZA67	90	105	~14	4.2
24	ZA68	90	105	~15	5.2
25	ZA71	90	105	~18	8.2
26	ZA72	90	105	~19	9.2
27	ZA73	90	105	~20	10.2
28	ZA74	90	105	~21	11.2
29	ZA75	90	105	~22	12.2
30	ZA76	90	105	~23	13.2
31	ZA77	90	105	~24	14.2
32	ZA78	90	105	~25	15.2
33	ZA81	90	105	~28	18.2
34	ZA82	90	105	~29	19.2
35	ZA83	90	105	~30	20.2
36	ZA84	90	105	~31	21.2
37	ZA85	90	105	~32	22.2
38	ZA86	90	105	~33	23.2
39	ZA87	90	105	~34	24.2
40	ZA88	90	105	~35	25.2

Table 2.2 Extrusion Condition.

2.3 Observation of microstructure and tensile test

The microstructure specimens are machined from as-extruded plate of normal direction and are polished by #400, #600, #800, #1000, #2000 and #4000, then polished with 0.3um and 0.05um alumina powder and etched in a picric-acetic solution (10ml acetic acid+4.2g picric acid+10ml H2O+70ml ethanol (95%))and then observed by optical microscopy(OM). Grain size is measured using the line intercept method.

2.4 Mechanical property

Tensile and compressive test are involved in mechanical properties at room temperature. The tensile specimens (Figure 2.4.1) are machined out from as-extruded plate with the tensile axis parallel to the extrusion direction. The Instron 5582 machine equipped with extensometer for accurate strain measurements is conducted on tensile and compressive tests. Cylindrical tensile specimens (4 mm in diameter and 16 mm in gauge length) and compressive specimens (8 mm in diameter and 12 mm in height) are cut along the extrusion direction. All tensile and compressive tests are performed at ambient temperature using a strain rate of 2×10^{-4}/s.

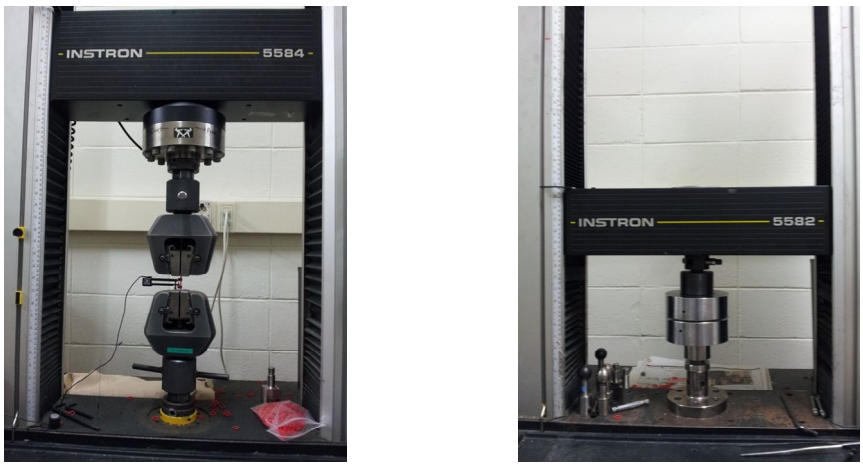

(a) (b)

Figure 2.4.1 (a) The Instron 5582 machine(Tensile Test) and (b) The Instron 5582 machine(Compressive Test).

2.5Mechanical Texture Measurement

The effect of Zn and Al content on the as-extruded texture and the changes in texture due to extrusion were systematically examined using the X-ray diffraction method by the X'pert pro XRD machine (Philips) with nickel-filtered copper target and the acceleration voltage and current were 40 kV and 30 mA respectively. For the texture measurement, extruded magnesium alloys were mechanically polished with sandpaper #4000 and then polished with 0.3μm alumina powder. A set of six pole figures $((0002),\{10\bar{1}0\},\{10\bar{1}1\},\{10\bar{1}2\},\{10\bar{1}3\}$ and $\{11\bar{2}0\})$ was collected and used to obtain the orientation distribution functions ODF (Orientation Distribution Function) calculated by the ADC (Arbitrarily Defined Cells) method of Labo Tex software after background removal and defocusing correction of the raw experimental data.

3. RESULT & DISCUSSION

3.1 Microstructure

Figure 3.1.1, 3.1.2, 3.1.3, 3.1.4, 3.1.5 show the microstructures of the as-extruded ZA alloys extruded at 340^{o}C observed from the ND planes. Generally the average grain size decrease slightly with the Zn or Al of alloying elements, and the average grain sizes determined by the linear intercept method were on the table 3.1, respectively. The phenomena observed in the case of magnesium alloys are the DRX, which improve the workability of the material at elevated temperatures. During the hot extrusion process, the occurred DRX plays an important part in refining the microstructure of the alloy. In these microstructures it is considered that DRX actively occurred with the addition of Zn and Al. Typically, from figure 3.1.6 when the content of Zn is fixed, the grain size of these six alloys is decreasing around from 7.10um to 5.22um regularly. Similar trend happens on other two series. In magnesium alloys, the precipitate acts as a nucleation site for recrystallized grains and prevents the grain growth by pinning effect. Therefore, the alloy with precipitates shows finer grain structures compared with the alloy without precipitates [31].

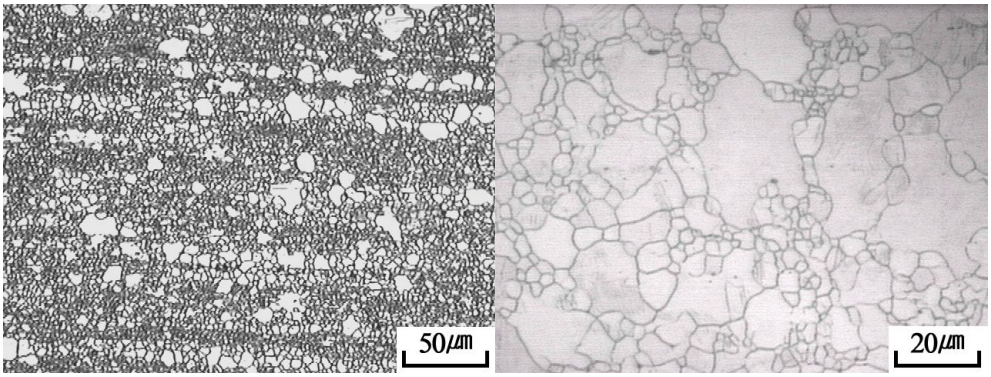

(a)

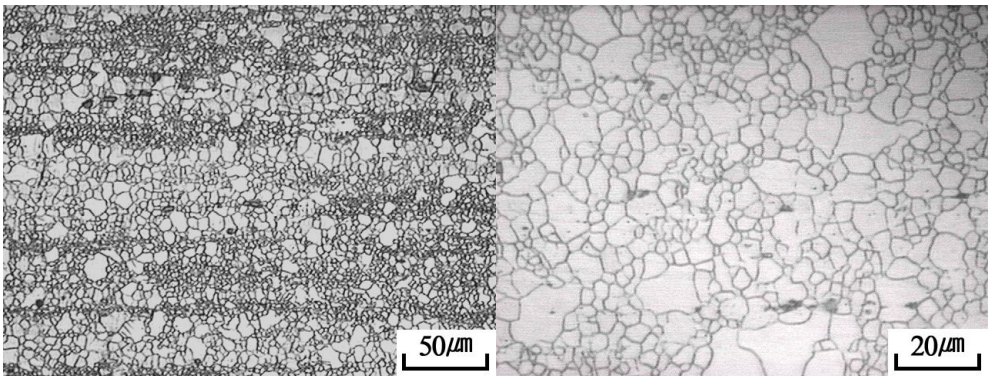

(b)

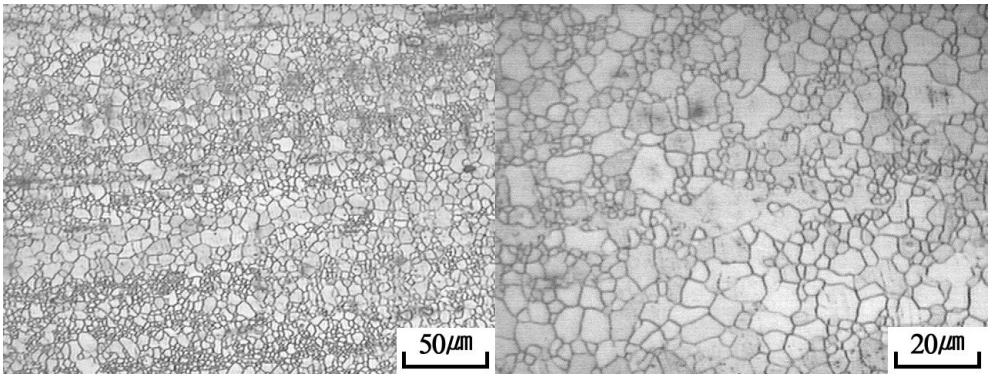

(c)

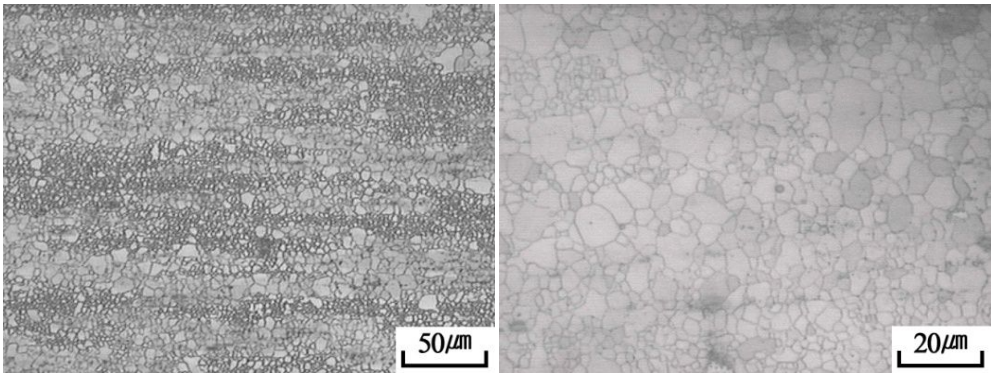

(d)

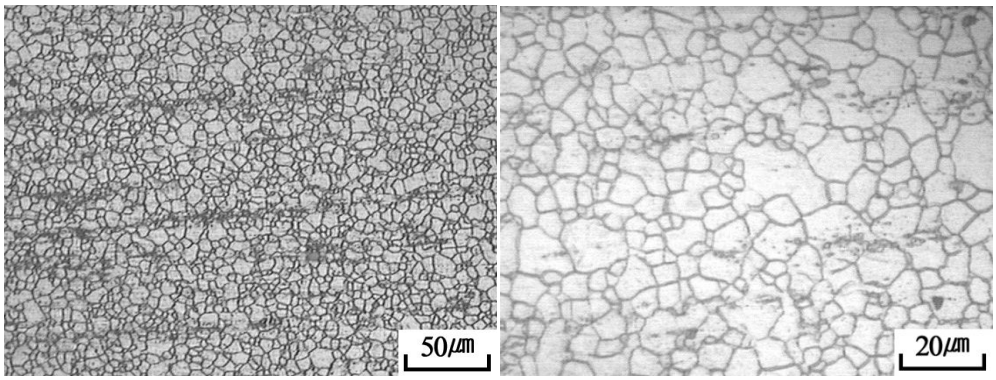

(e)

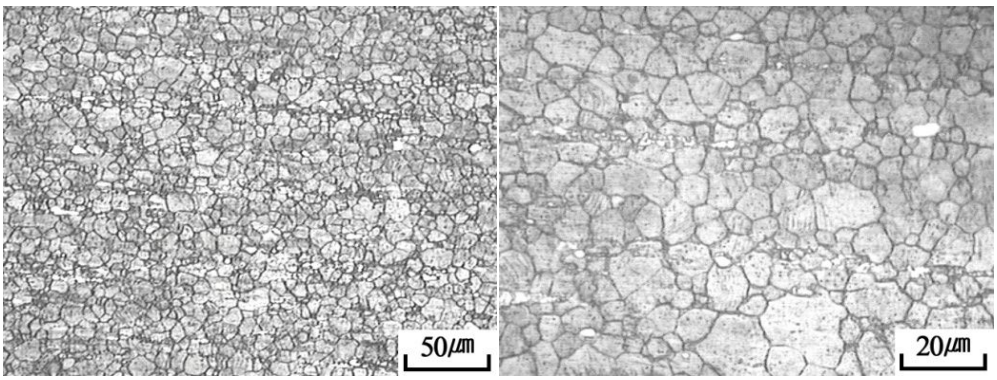

(f)

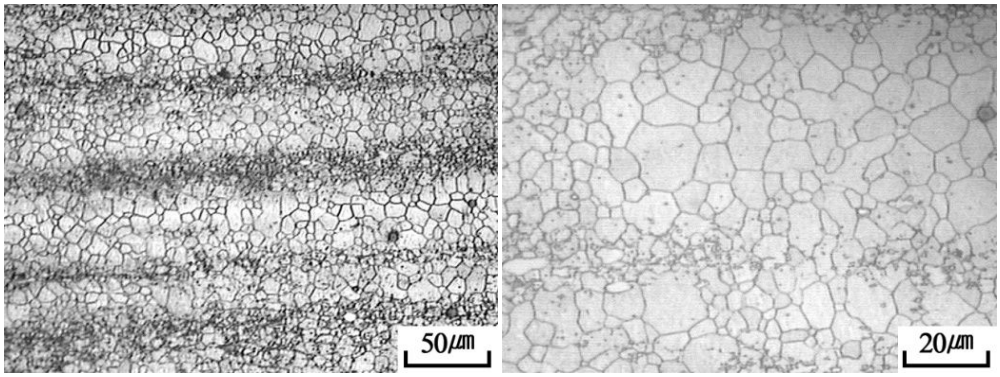

(g)

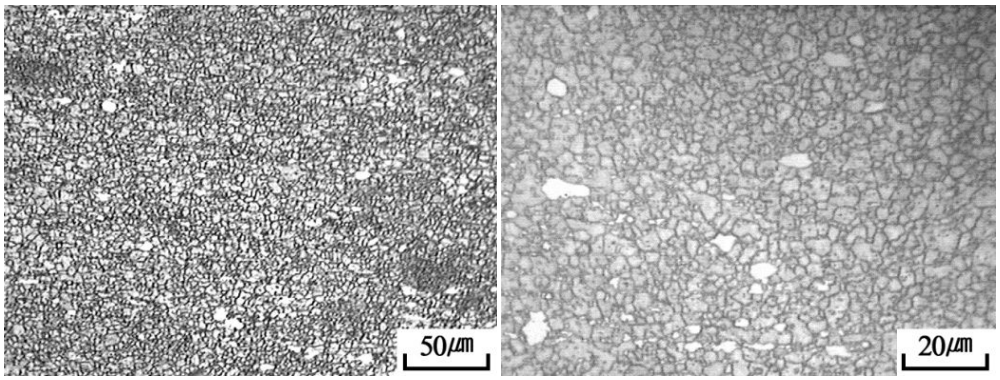

(h)

Figure 3.1.1 Optical micrographs of the as-extruded Mg-Zn-Al alloys; (a) ZA41, (b) ZA42, (c) ZA43, (d) ZA44, (e) ZA45, (f) ZA46, (g) ZA47, (h) ZA48.

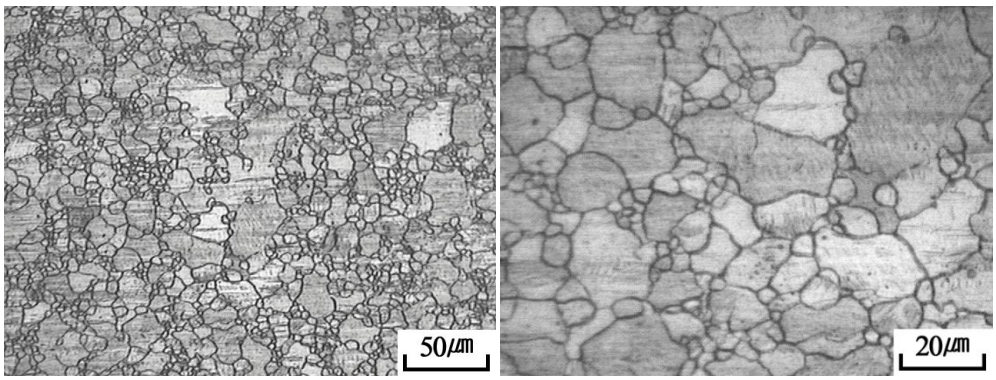

(a)

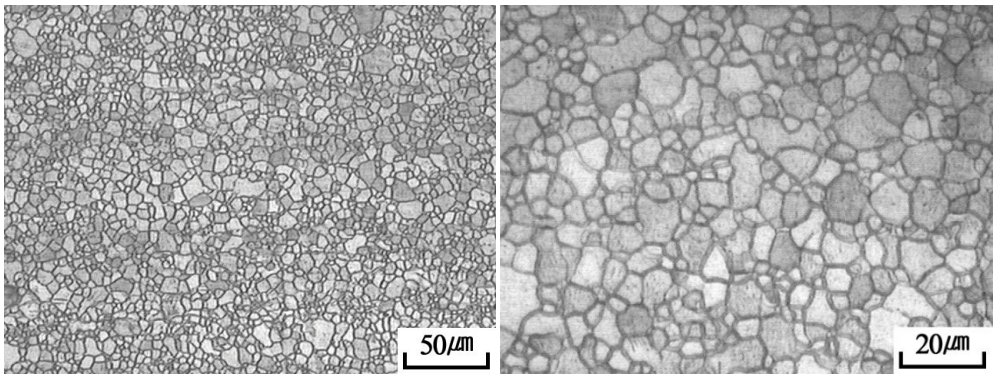

(b)

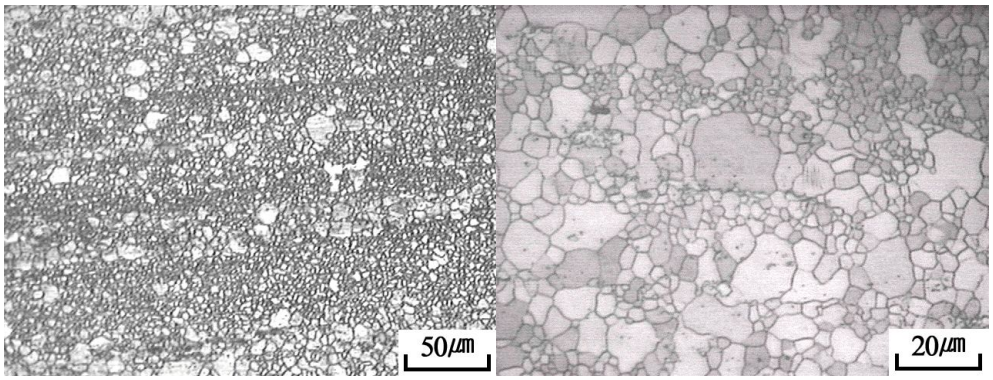

(c)

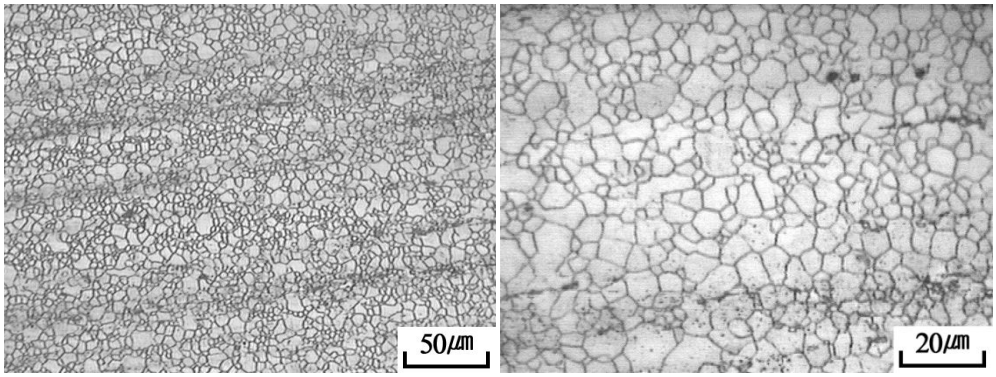

(d)

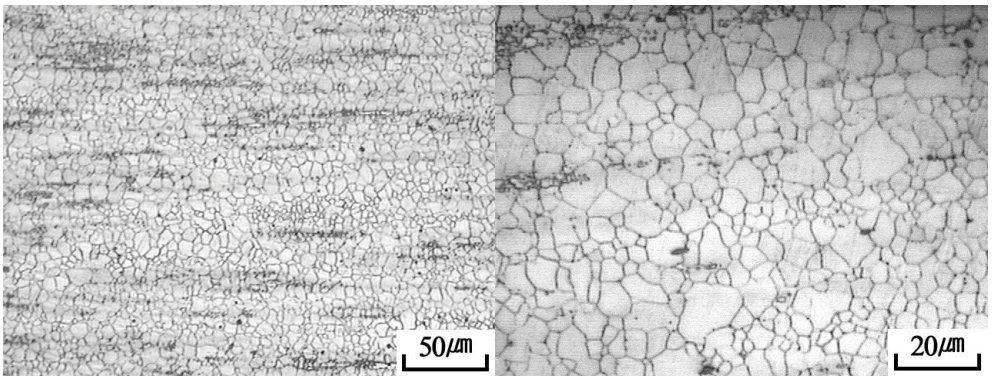

(e)

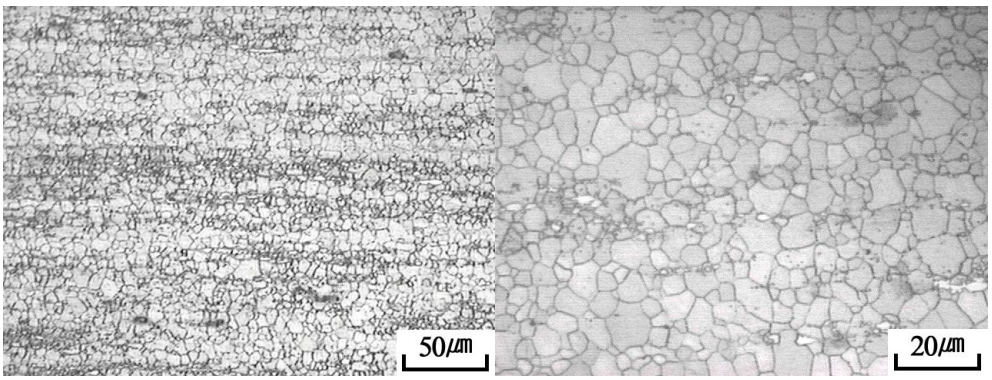

(f)

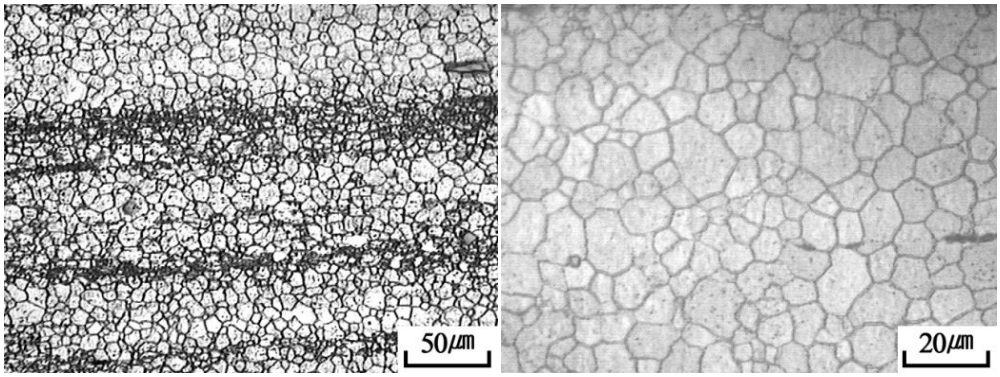

(g)

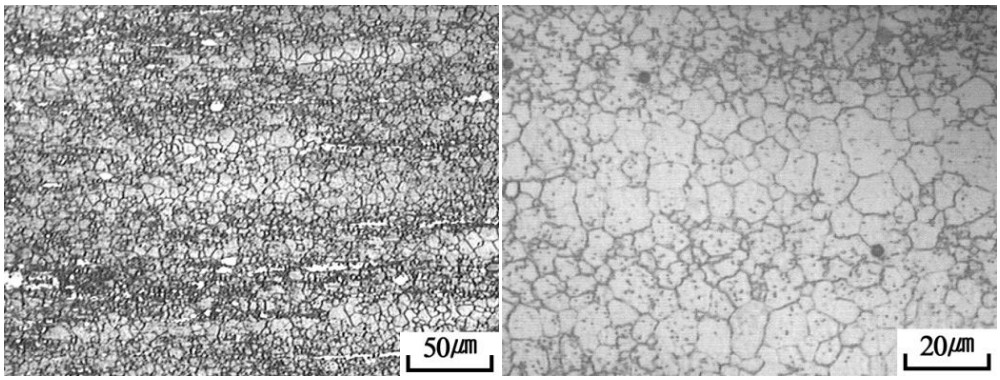

(h)

Figure 3.1.2 Optical micrographs of the as-extruded Mg-Zn-Al alloys; (a) ZA51, (b) ZA52, (c) ZA53, (d) ZA54, (e) ZA55, (f) ZA56, (g) ZA57, (h) ZA58.

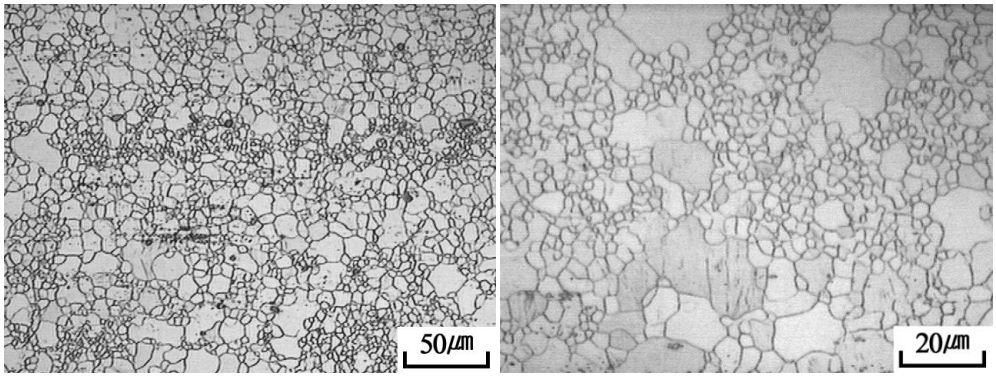

(a)

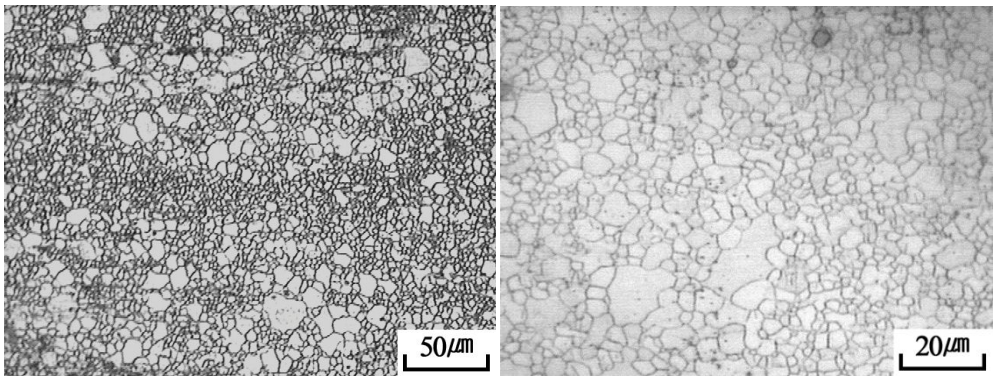

(b)

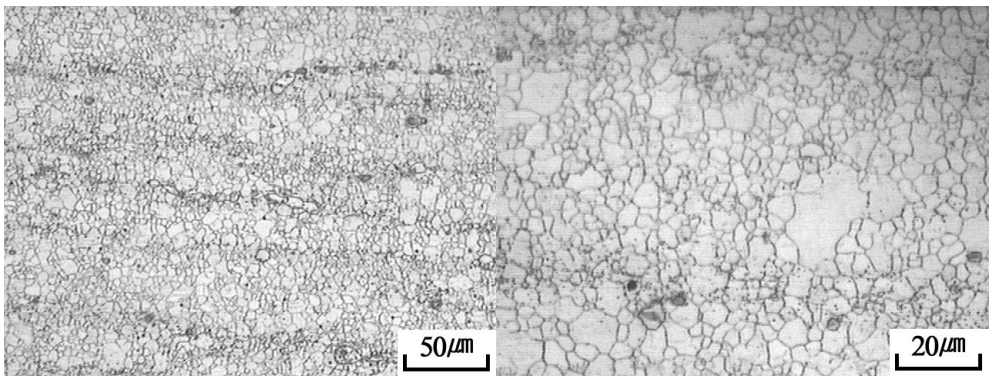

(c)

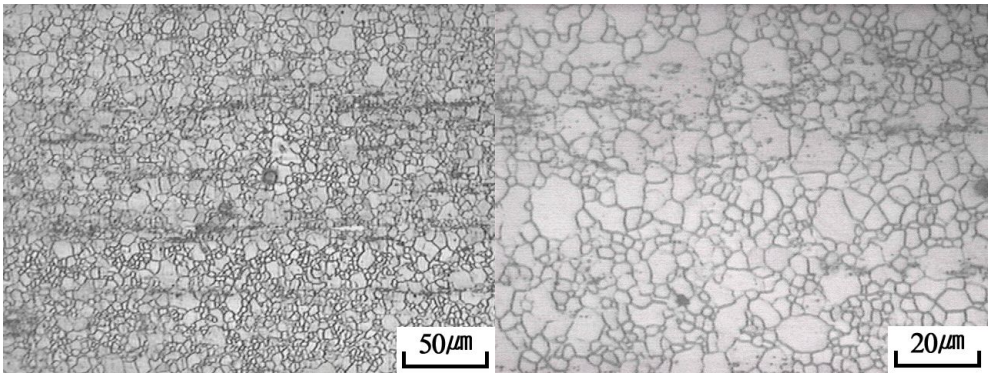

(d)

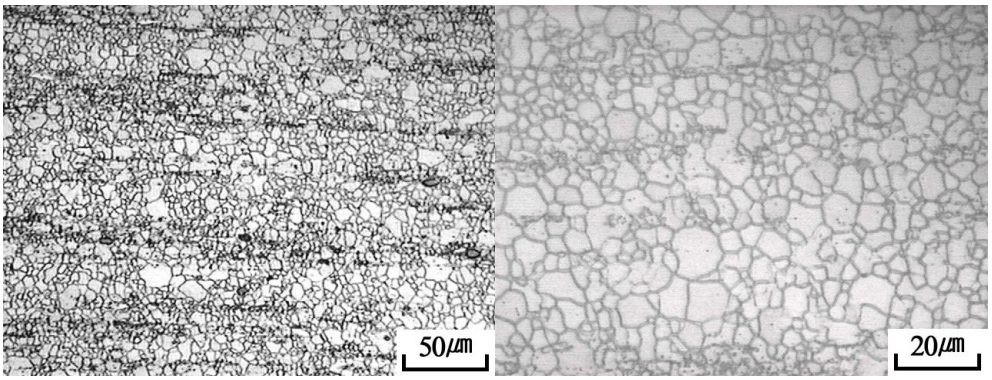

(e)

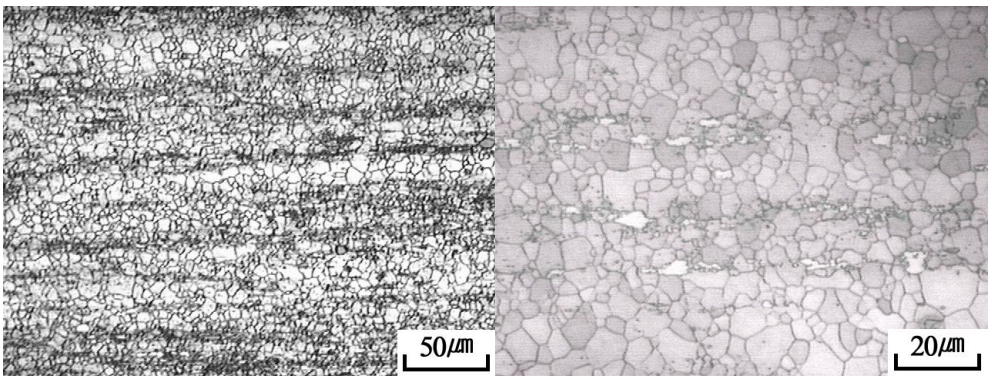

(f)

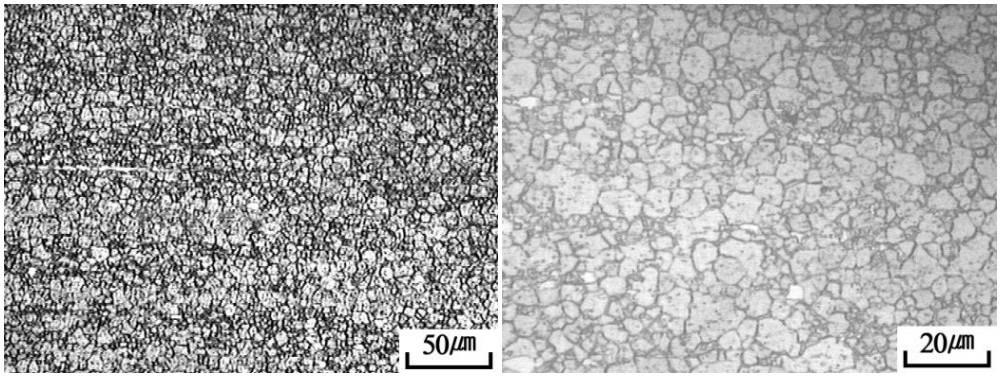

(g)

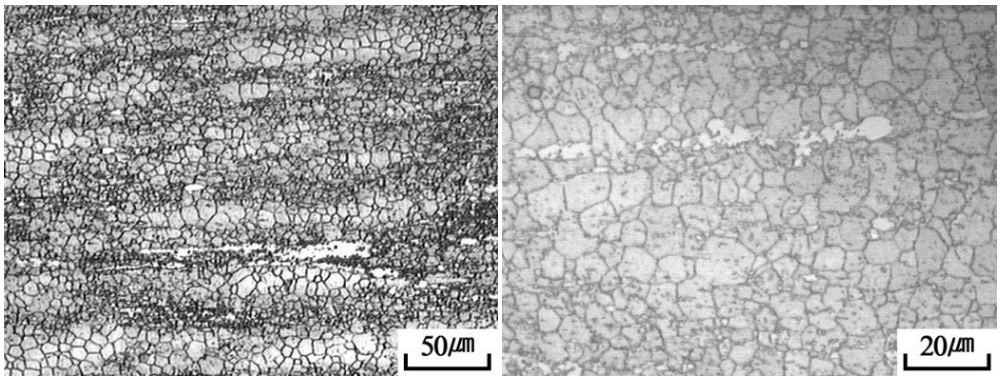

(h)

Figure 3.1.3 Optical micrographs of the as-extruded Mg-Zn-Al alloys; (a) ZA61, (b) ZA62, (c) ZA63, (d) ZA64, (e) ZA65, (f) ZA66, (g) ZA67, (h) ZA68.

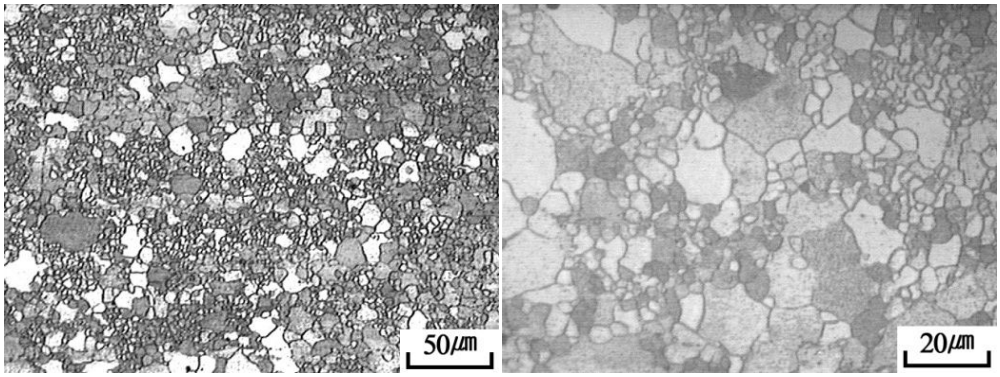

(a)

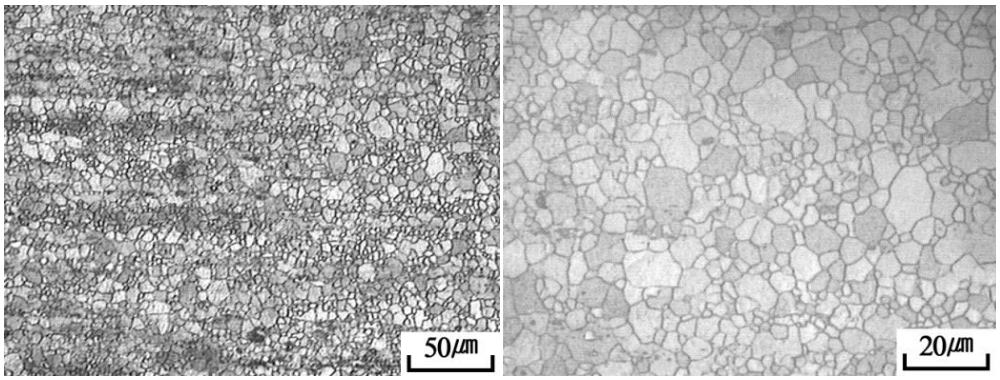

(b)

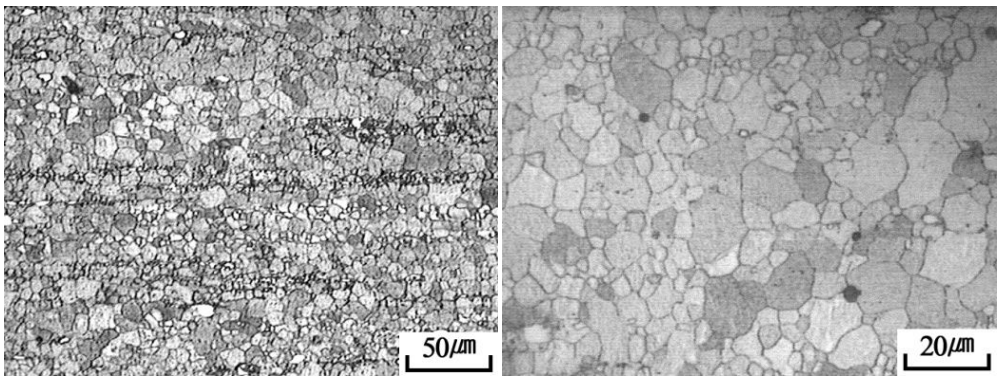

(c)

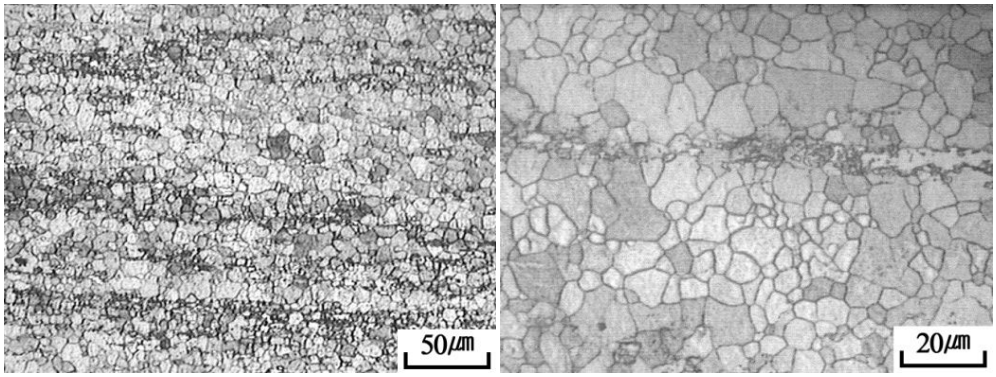

(d)

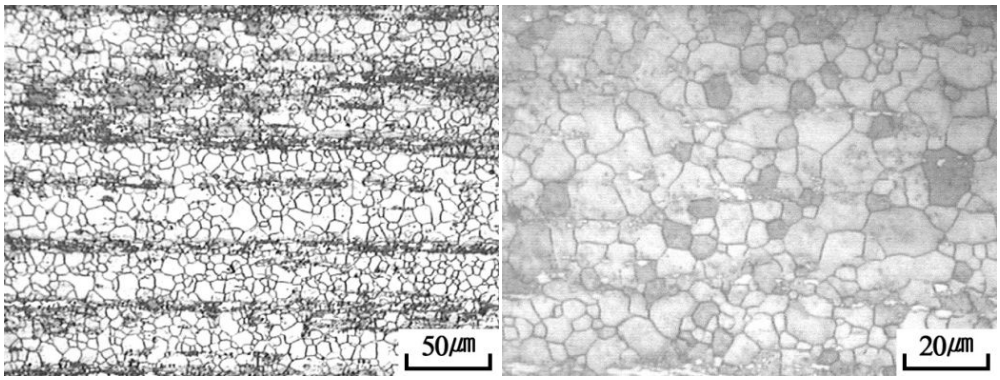

(e)

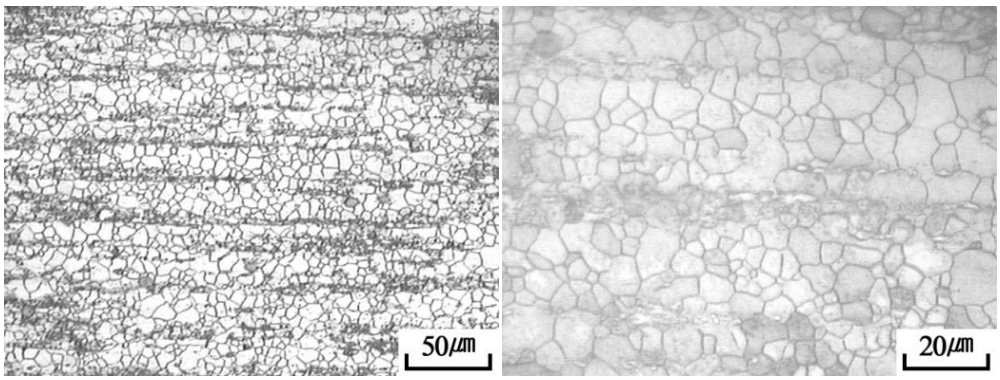

(f)

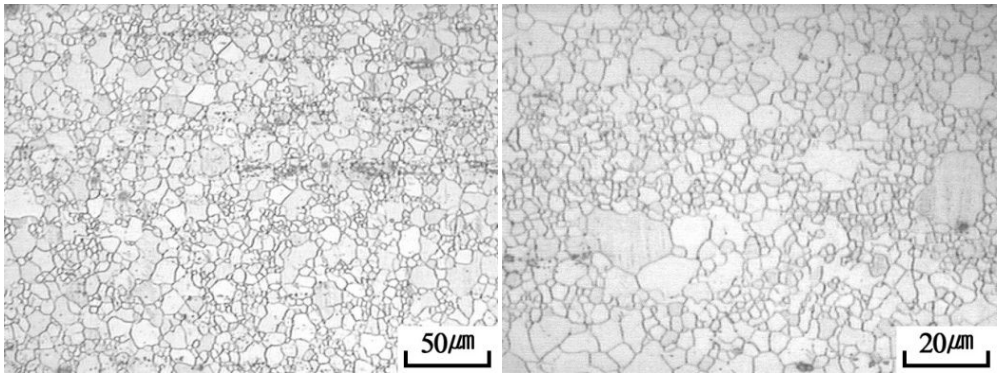

(g)

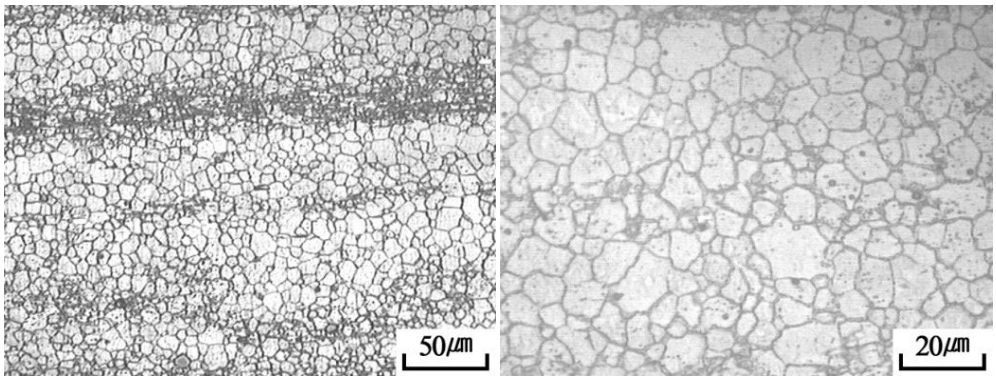

(h)

Figure 3.1.4 Optical micrographs of the as-extruded Mg-Zn-Al alloys; (a) ZA71, (b) ZA72, (c) ZA73, (d) ZA74, (e) ZA75, (f) ZA76, (g) ZA77, (h) ZA78.

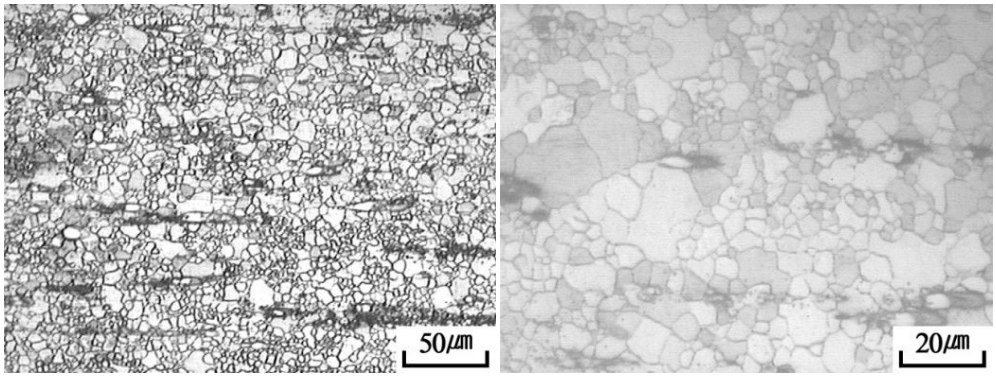

(a)

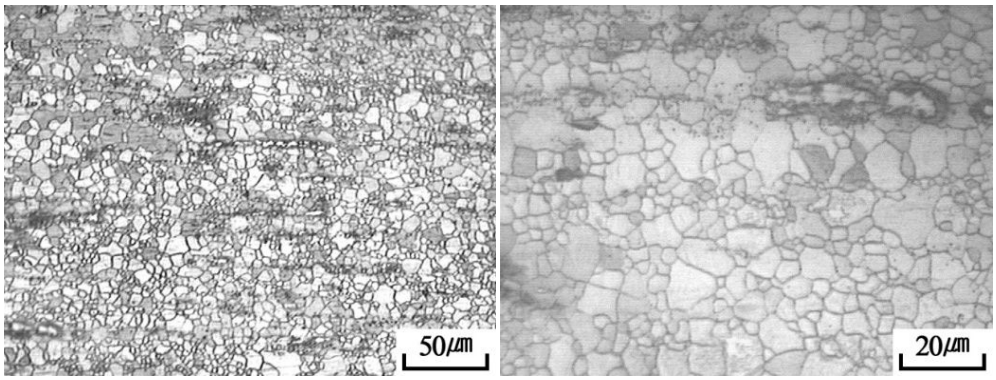

(b)

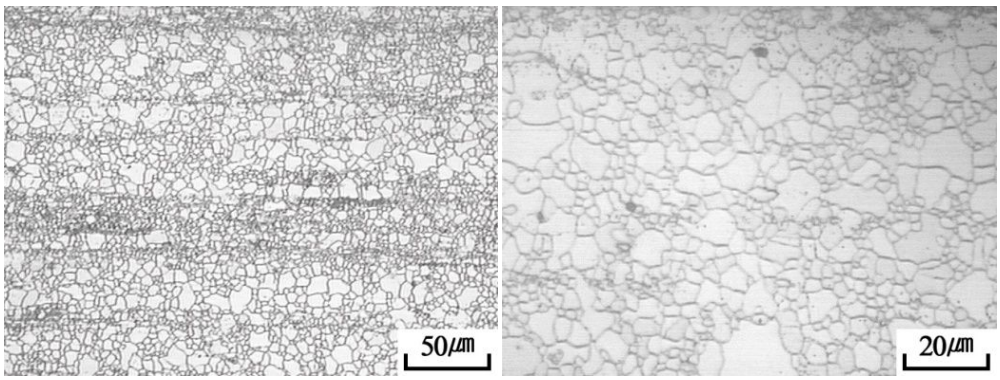

(c)

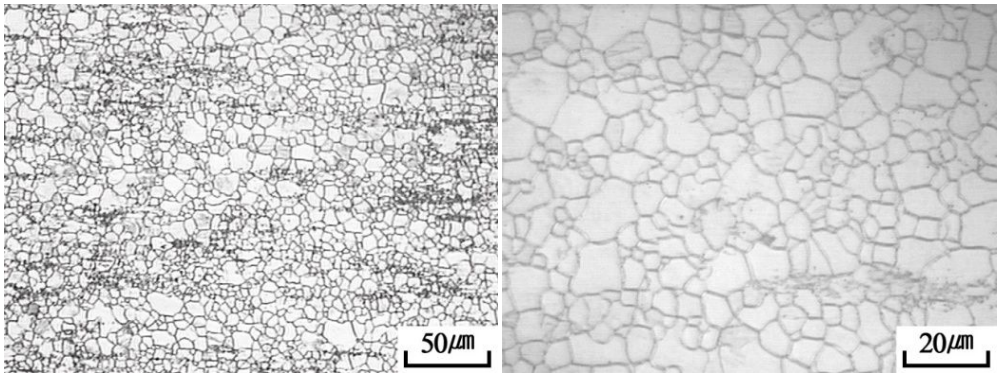

(d)

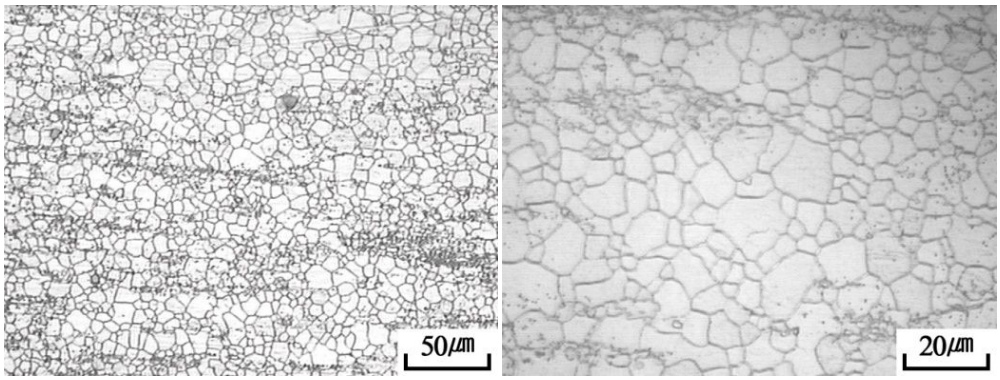

(e)

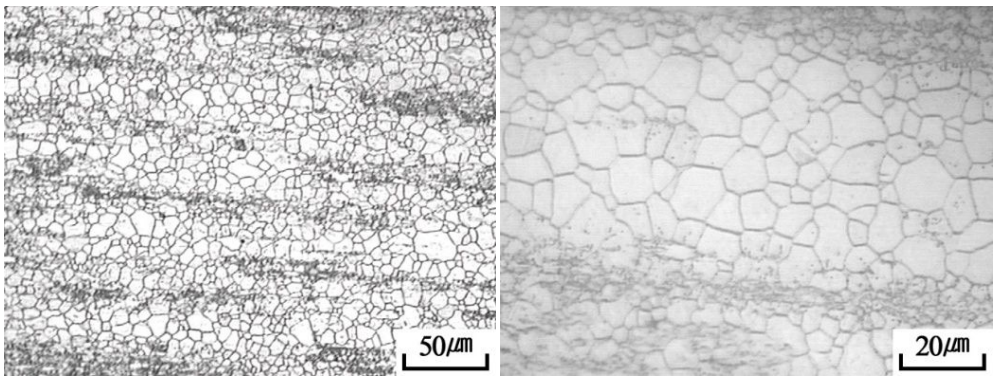

(f)

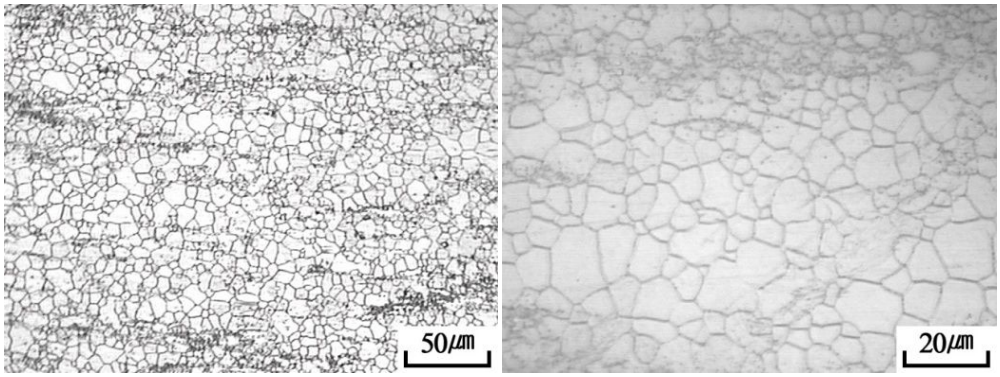

(g)

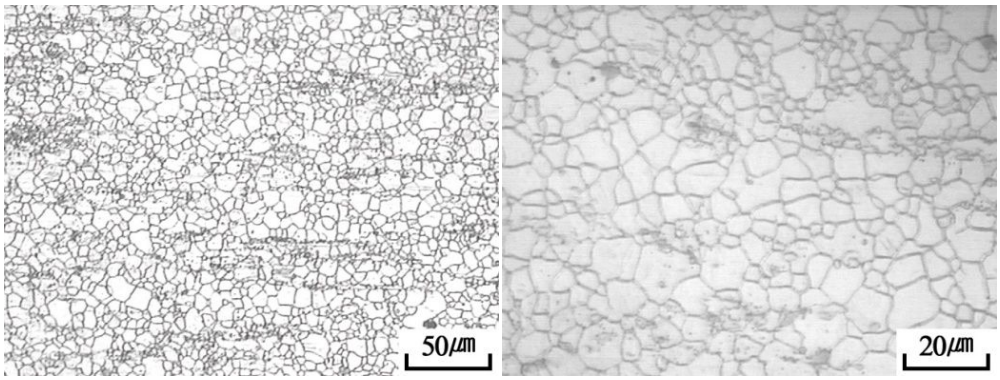

(h)

Figure 3.1.5 Optical micrographs of the as-extruded Mg-Zn-Al alloys; (a) ZA81, (b) ZA82, (c) ZA83, (d) ZA84, (e) ZA85, (f) ZA86, (g) ZA87, (h) ZA88.

Alloy	Grain Size (µm)	Alloy	Grain Size (µm)	Alloy	Grain Size (µm)	Alloy	Grain Size (µm)	Alloy	Grain Size (µm)
ZA41	8.5	ZA51	8.3	ZA61	7.8	ZA71	8.5	ZA81	7.2
ZA42	6.3	ZA52	5.9	ZA62	5.0	ZA72	8.0	ZA82	6.5
ZA43	5.0	ZA53	5.0	ZA63	4.4	ZA73	6.7	ZA83	5.2
ZA44	4.7	ZA54	4.5	ZA64	4.0	ZA74	6.0	ZA84	5.0
ZA45	4.5	ZA55	4.2	ZA65	3.7	ZA75	5.2	ZA85	4.6
ZA46	4.1	ZA56	4.0	ZA66	3.5	ZA76	4.6	ZA86	4.1
ZA47	4.3	ZA57	3.8	ZA67	3.2	ZA77	4.2	ZA87	3.6
ZA48	4.0	ZA58	4.0	ZA68	3.0	ZA78	3.8	ZA88	3.2

Table 3.1 Average Grain Size of Microstructure of These Alloys.

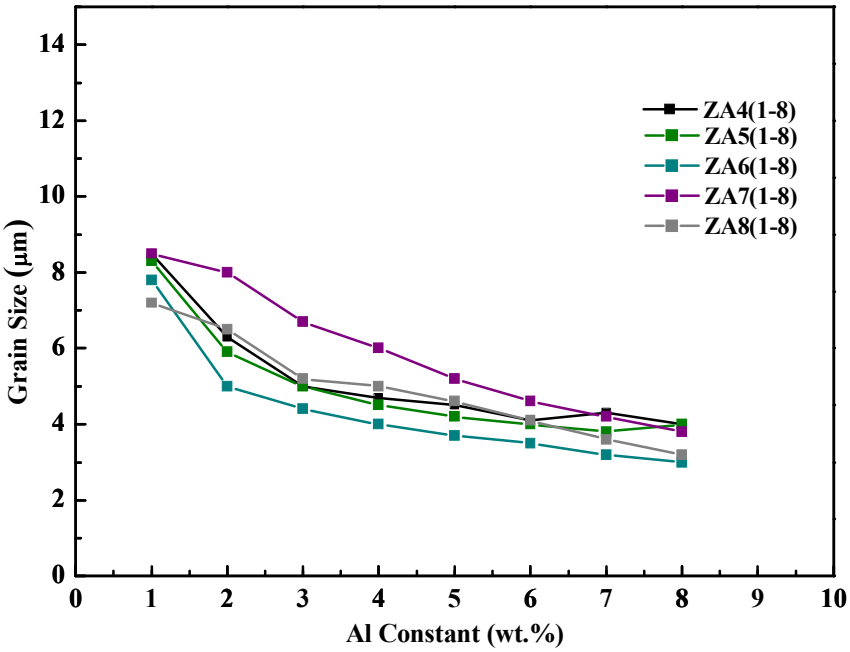

Figure 3.1.6 Average Grain Size Curve of Microstructure of These Alloys.

3.2 Mechanical Properties and Textrues

3.2.1 Mechanical properties of ZA41-ZA48 alloys extruded at 340℃

Figure 3.2.1~ Figure 3.2.4 show that the tensile and compressive properties of Mg-4Zn-y (y=1~8) alloys extruded at 340^{o}C. When the 1 wt.%Al was added to the ZA41 alloy, the U.T.S. and Y.S. were increased by the solid solution strengthening and grain refinement with addition of Al. Like general, it is expected that if Al is added to the ZA41 alloy, the mechanical property should be increased by solid solution hardening. The compressive flow curves represented the s-shaped curves that originated from the activation of the tensile twin at an initial stage of compressive deformation. From the results, the tensile and compressive behavior is similar to the commercial wrought magnesium alloys having basal texture and the mechanical properties of those alloys were increased with addition of Al to the ZA41 alloys due to the solid solution strengthening and grain refinement.

In Figure 3.2.5, the yield strength anisotropy of as-extruded ZA41-ZA48 are plotted. The results show that in the case of the ZA41-ZA48 alloys, the yield strength anisotropy of those alloys is close to 1.0. This means that the difference of yield strength in compression and tension of extrusions is decreased. As mentioned above, yield strength anisotropy is caused by activated tension twin and also in the case of magnesium alloys having very fined grains, twinning is hardly activated in the plastic deformation of magnesium alloys [32, 33].

In order to understand the effect of Zn and Al content on the deformation behavior, the textures of the ZA alloys were examined in the as-extruded condition. The textures of the as-extruded ZA alloys are illustrated in Figure 3.2.6 with the pole figures. The (0002) planes were found to be nearly parallel to the normal plane of the extruded plates which showed the general characteristics of the extrusion texture of Mg alloys, but the

(0002) poles were slightly split into the extrusion directions. It is found that the basal poles of ZA41 ZA44 ZA48 are parallel to the normal direction, with a slight tendency to incline toward the extrusion direction. In this graph, the basal pole intensities were plotted. The peak intensity positions are about 15~30o away from the normal direction to the extrusion direction and the intensities were nearly zero after 45o.From this tensile curve, the ZA41 elongation is bigger than ZA44, and ZA48. This is because that the ZA41 basal pole shows a stronger tendency to incline toward the extrusion direction than ZA44 and ZA48. With the tendency decreasing, the ductility is becoming poor.

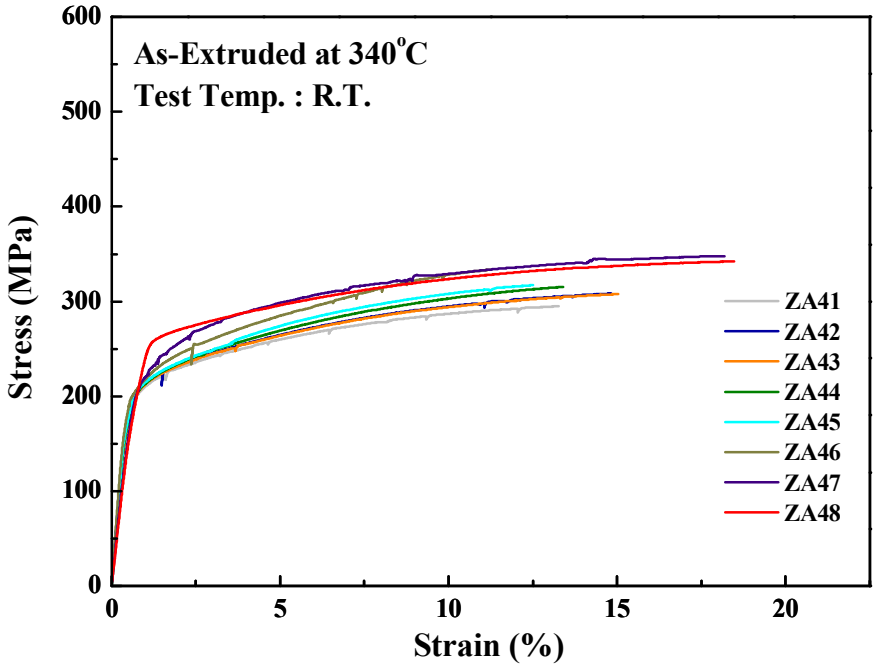

Figure 3.2.1 Tensile stress-strain curves of ZA41-ZA48 alloys extruded at 340°C.

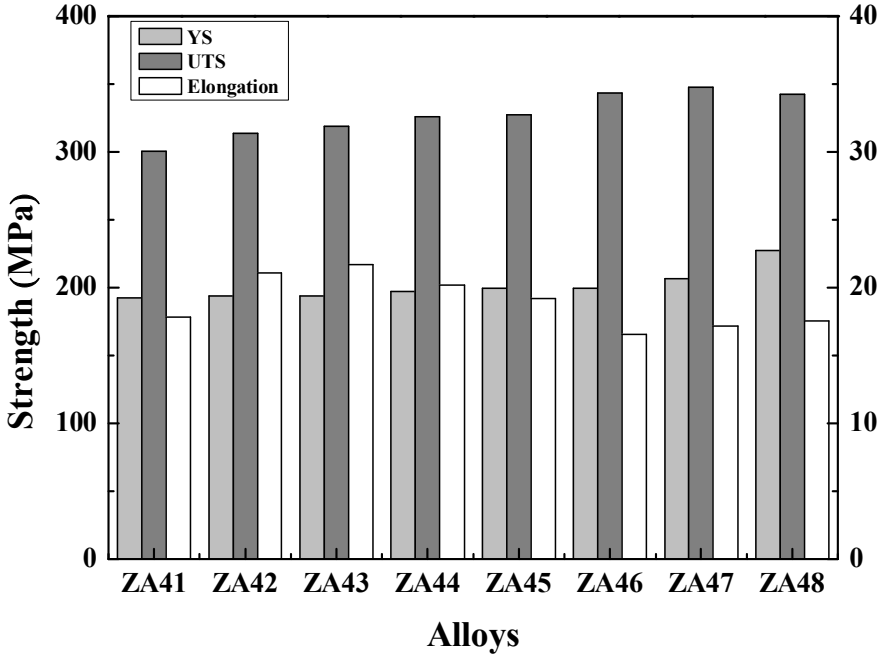

Figure 3.2.2 U.T.S , Y.S. and elongation on tensile test of ZA41-ZA48 alloys extruded at 340^{o}C.

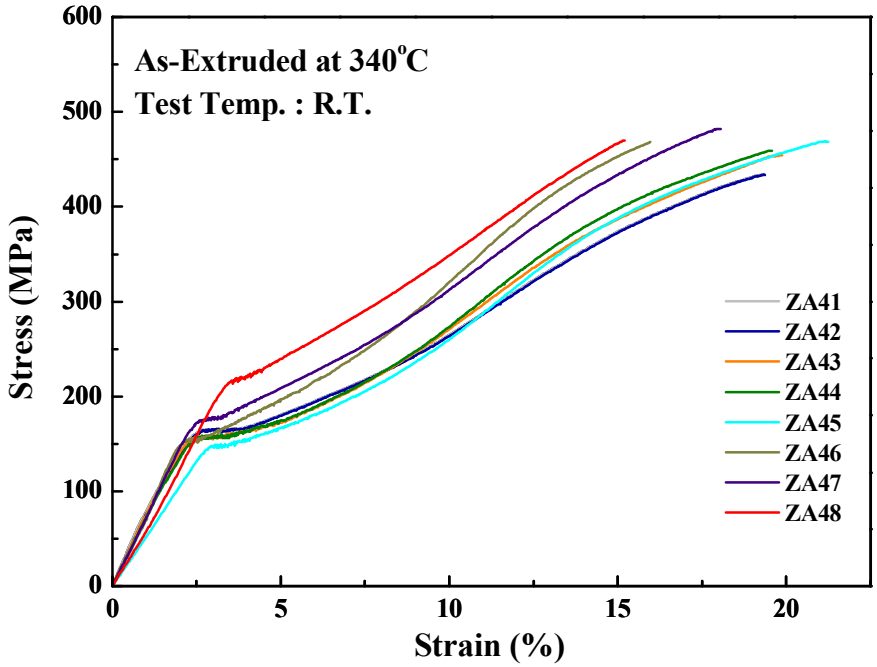

Figure 3.2.3 Compression stress-strain curves of ZA41-ZA48 alloys extruded at 340°C.

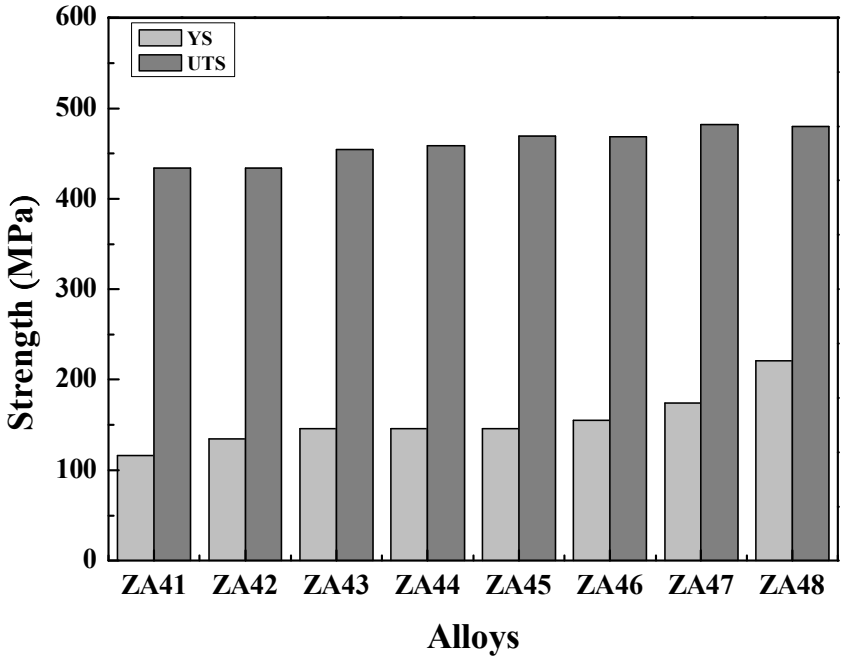

Figure 3.2.4 U.T.S , Y.S. and elongation on compression test of ZA41-ZA48 alloys extruded at 340^{o}C.

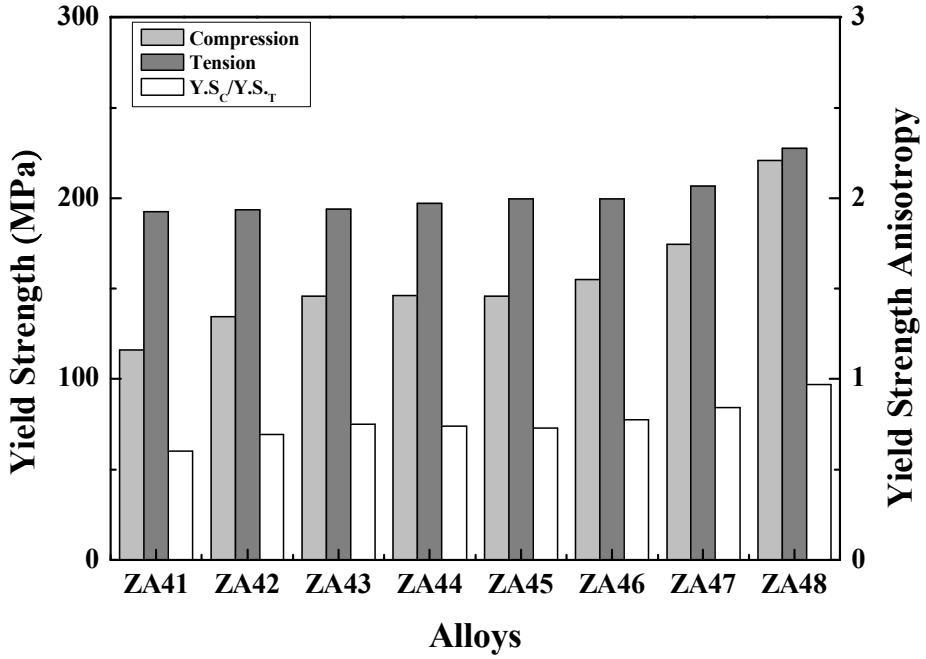

Figure 3.2.5 Figure Yield Strength Anisotropy of ZA41-ZA48 Alloys Extruded at 340^{o}C.

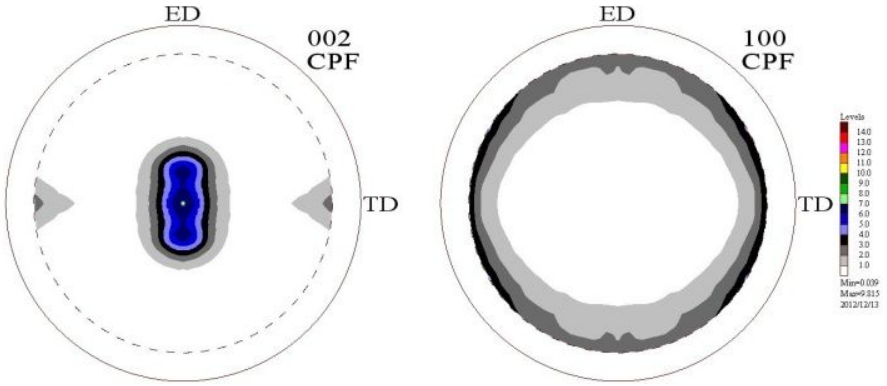

(a)

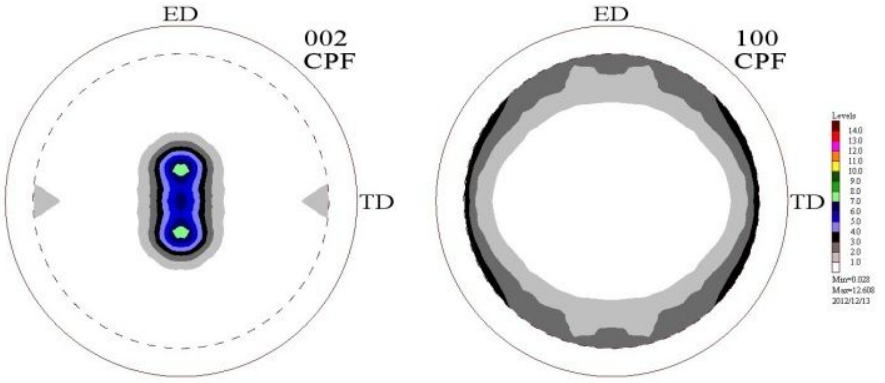

(b)

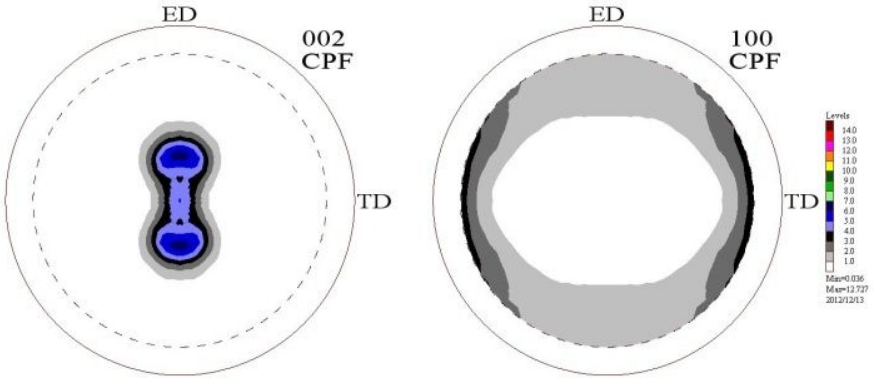

(c)

Figure 3.2.6 Pole figures of ZA alloys extruded at 340^{o}C;

(a) ZA41, (b) ZA44, (c) ZA48 alloy.

3.2.2 Mechanical properties of ZA51-ZA58 alloys extruded at 340 ^{o}C.

Figure 3.2.7~ Figure 3.2.10 show that the tensile and compressive properties of Mg-5Zn-y (y=1~8) alloys extruded at 340^{o}C. With the content of Al increasing by 1 wt.%Al to the ZA51 alloy, the U.T.S. and Y.S. were increased by the solid solution strengthening and grain refinement with addition of Al. The compressive flow curves represented the s-shaped curves that originated from the activation of the tensile twin at an initial stage of compressive deformation. From the results, the tensile and compressive behavior is similar to the commercial wrought magnesium alloys having basal texture and the mechanical properties of those alloys were increased with addition of Al to the ZA51 alloys due to the solid solution strengthening and grain refinement. Like general, it is expected that if Al is added to the ZA41 alloy, the mechanical property should be increased by solid solution hardening.

In Figure 3.2.11, the yield strength anisotropy of as-extruded ZA51-ZA58 are plotted. The results show that in the case of the ZA51-ZA58 alloys, the yield strength anisotropy of those alloys is close to 1.0. This means that the difference of yield strength in compression and tension of extrusions is decreased. As mentioned above, yield strength anisotropy is caused by activated tension twin and also in the case of magnesium alloys having very fined grains, twinning is hardly activated in the plastic deformation of magnesium alloys [32, 33].

In order to understand the effect of Zn and Al content on the deformation behavior, the textures of the ZA alloys were examined in the as-extruded condition. The textures of the as-extruded ZA alloys are illustrated in Figure 3.2.12 with the pole figures. The (0002) planes were found to be nearly parallel to the normal plane of the extruded plates which showed the general characteristics of the extrusion texture of Mg alloys, but the (0002) poles were slightly split into the extrusion directions.

With the Al increasing, the tendency inclined to extrusion direction decrease. The maximum intensity moving toward the center. From this graph, the peak Intensity

position of ZA51 and ZA54 basal poles is near 20o. But the peak intensity position of ZA58 is closed to 7. With the similar trend of ZA4y, the tendency inclined to extrusion direction decrease and the tendency inclined to normal direction increasing with the Al increasing. From this tensile curve, also the ZA51 has greater tensile elongation than ZA54, and ZA58. This also can prove that with the basal pole tendency inclined to extrusion direction decreasing. The alloys elongation is decreasing.

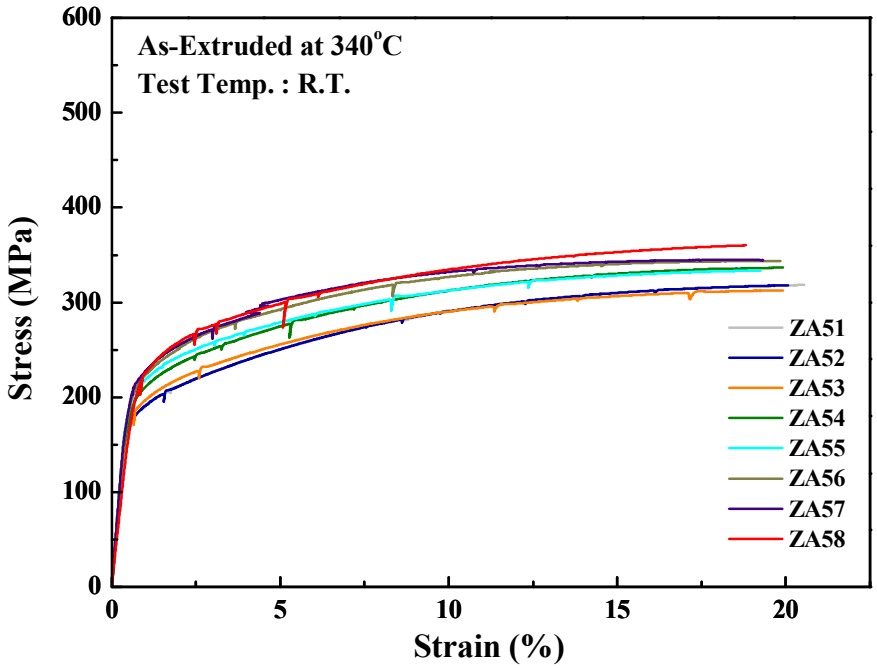

Figure 3.2.2 Tensile stress-strain curves of ZA51-ZA58 alloys extruded at 340°C.

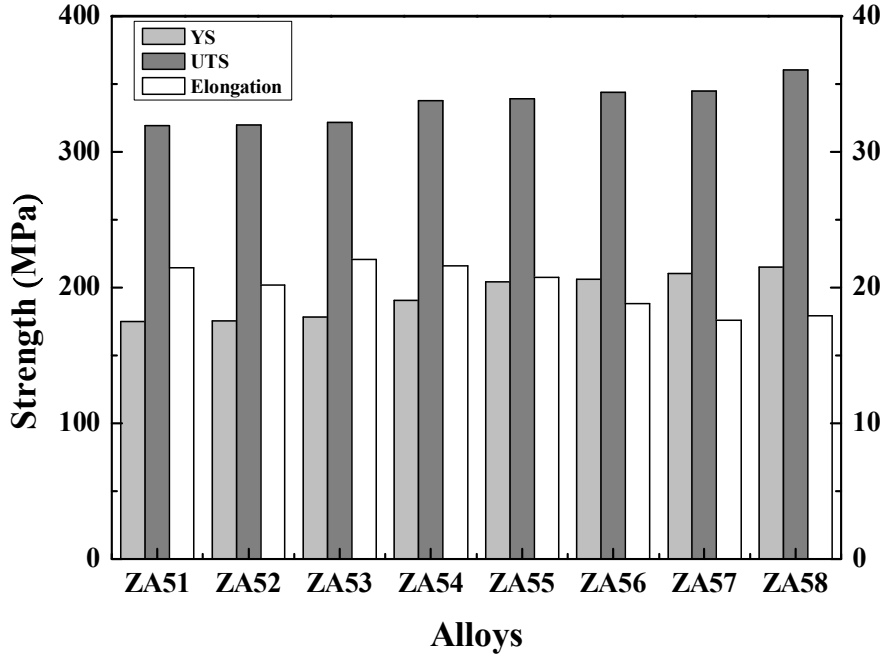

Figure 3.2.8 U.T.S, Y.S and elongation on tensile test of ZA51-ZA58 alloys extruded at 340^{o}C.

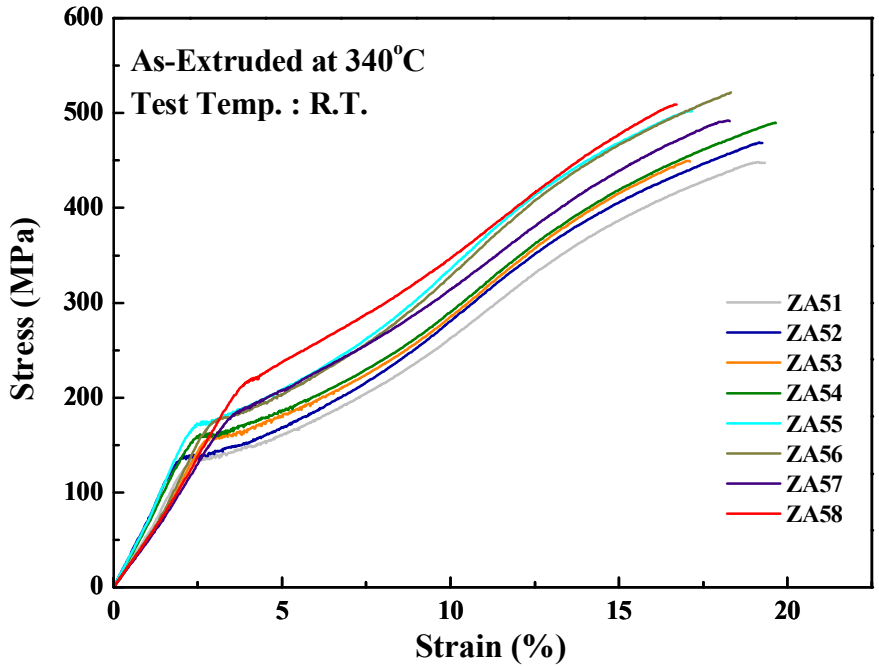

Figure 3.2.9 Compression stress-strain curves of ZA51-ZA58 alloys extruded at 340℃.

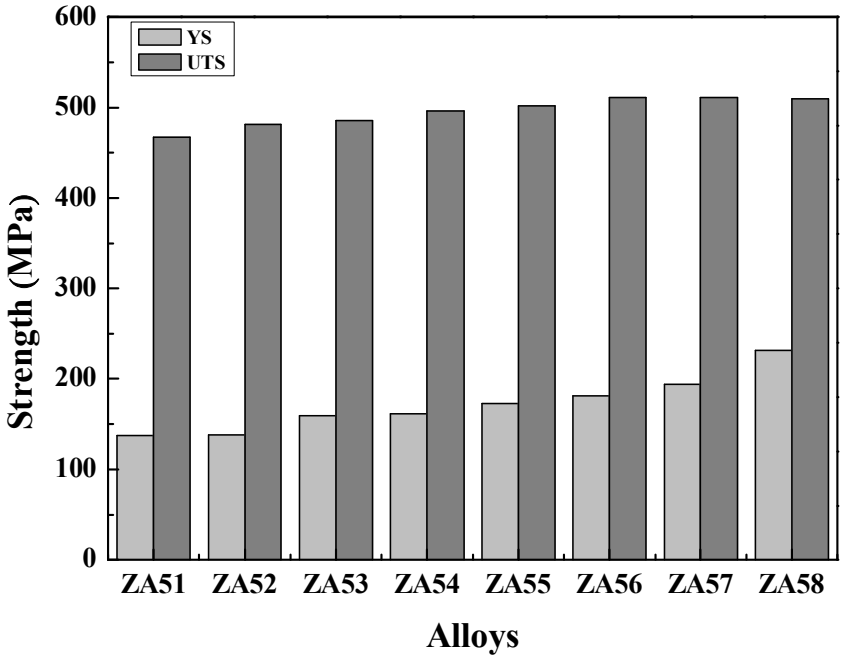

Figure 3.2.10 U.T.S, Y.S. and elongation on compression test of ZA51-ZA58 alloys extruded at 340℃.

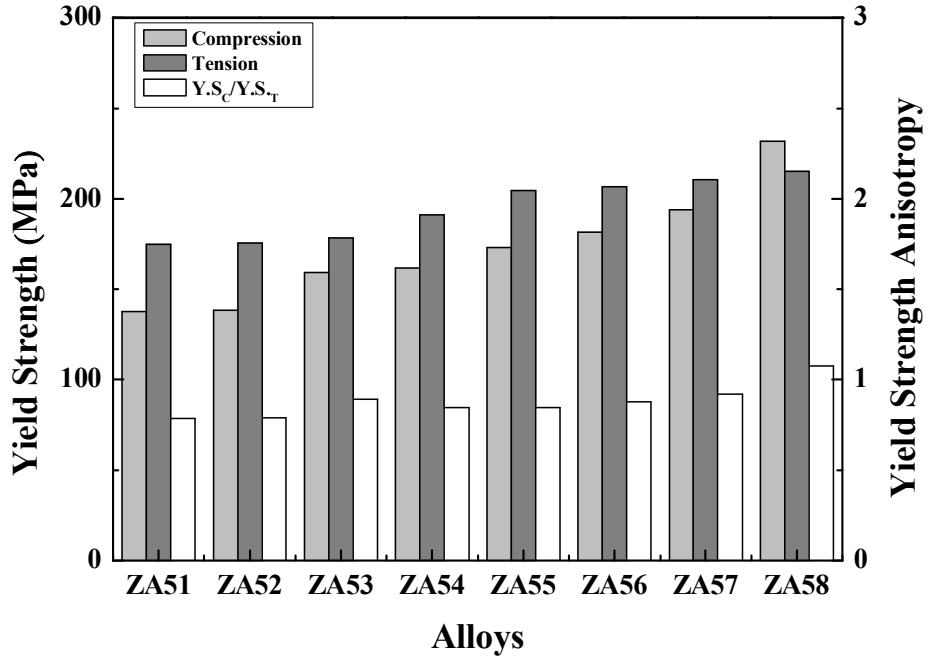

Figure 3.2.11 Yield Strength Anisotropy of ZA51-ZA58 Alloys Extruded at 340℃.

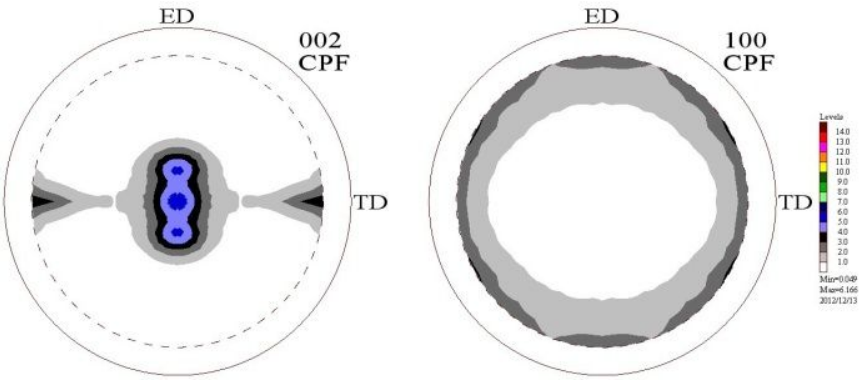

(a)

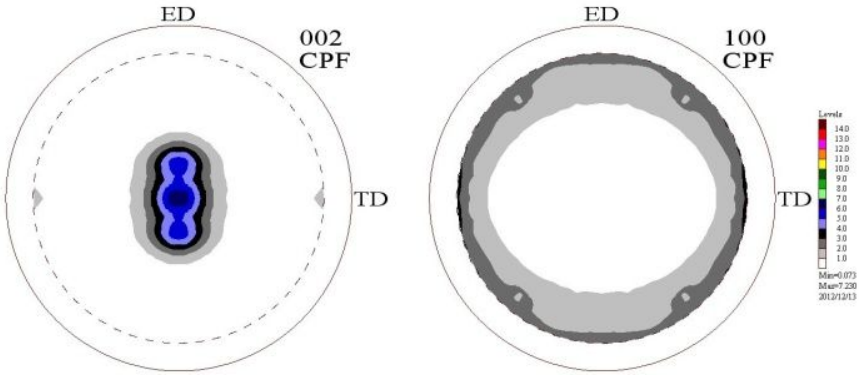

(b)

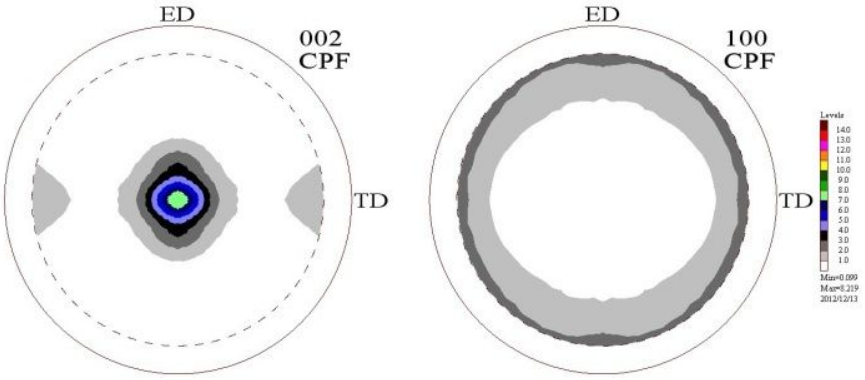

(c)

Figure 3.2.12 Pole figures of ZA alloys extruded at 340^{o}C;

(a) ZA51, (b) ZA54, (c) ZA58 alloy

3.2.3 Mechanical properties of ZA61-ZA68 alloys extruded at 340℃.

Figure 3.2.13 ~ Figure 3.2.16 are obtained for the tensile and compressive properties of Mg-6Zn-y (y=1~8)Al alloys extruded at 340℃. In the whole view, the YS and UTS is growing slightly as the Al content added increasingly just similar to the trend of ZA4y and ZA5y alloys above. In the tensile test, ZA63 shows the best elongation with 21.33%, and ZA65 shows a better mechanical property with YS 213.17Mpa, UTS 341.12Mpa and Elongation 20.32%. The strain hardening exponent of tensile test also shows a down trend from 0.223 to 0.191. From the results, the tensile and compressive behavior is similar to the commercial wrought magnesium alloys and the mechanical properties of those alloys were increased with addition of Al due to the solid solution strengthening and grain refinement.

In Figure 3.2.17, the yield strength anisotropy of as-extruded ZA61-ZA68 are plotted. The results show that in the case of the ZA61-ZA68 alloys, the yield strength anisotropy of those alloys is close to 1.0. This means that the difference of yield strength in compression and tension of extrusions is decreased. As mentioned above, yield strength anisotropy is caused by activated tension twin and also in the case of magnesium alloys having very fined grains, twinning is hardly activated in the plastic deformation of magnesium alloys [32, 33].

In order to understand the effect of Zn and Al content on the deformation behavior, the textures of the ZA alloys were examined in the as-extruded condition. The textures of the as-extruded ZA alloys are illustrated in Figure 3.2.18 with the pole figures. The (0002) planes were found to be nearly parallel to the normal plane of the extruded plates which showed the general characteristics of the extrusion texture of Mg alloys, but the (0002) poles were slightly split into the extrusion directions.

With the addition element increasing, the maximum intensity increase slightly. Also, in the tensile curve, the yield strength is increasing with Al increasing. Based on this , it is assumed that, the higher maximum intensity in basal pole, the stronger Yield

strength is. The decreasing grain size in microstructures also follow the tendency as well.

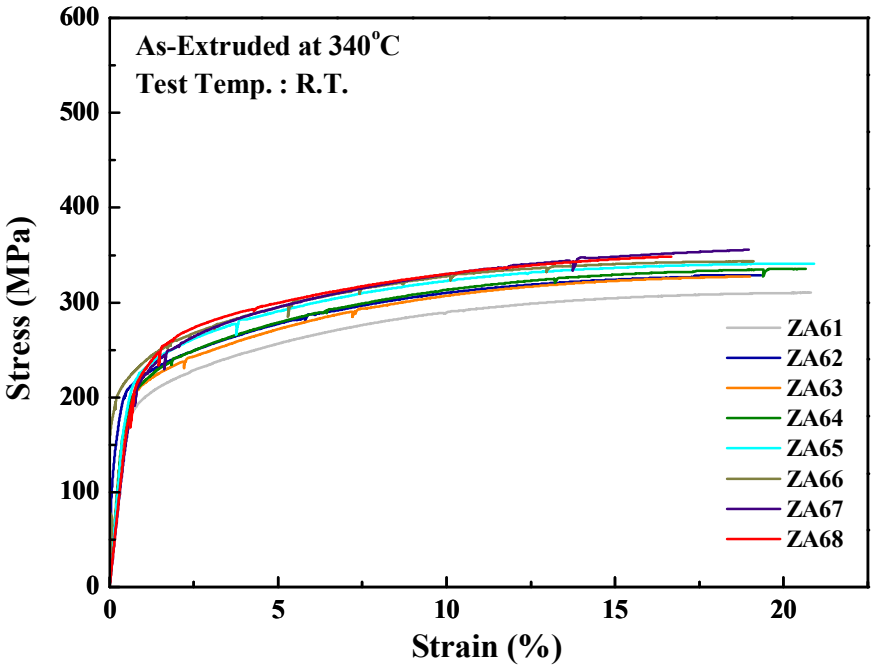

Figure 3.2.3 Tensile stress-strain curves of ZA61-ZA68 alloys extruded at 340°C.

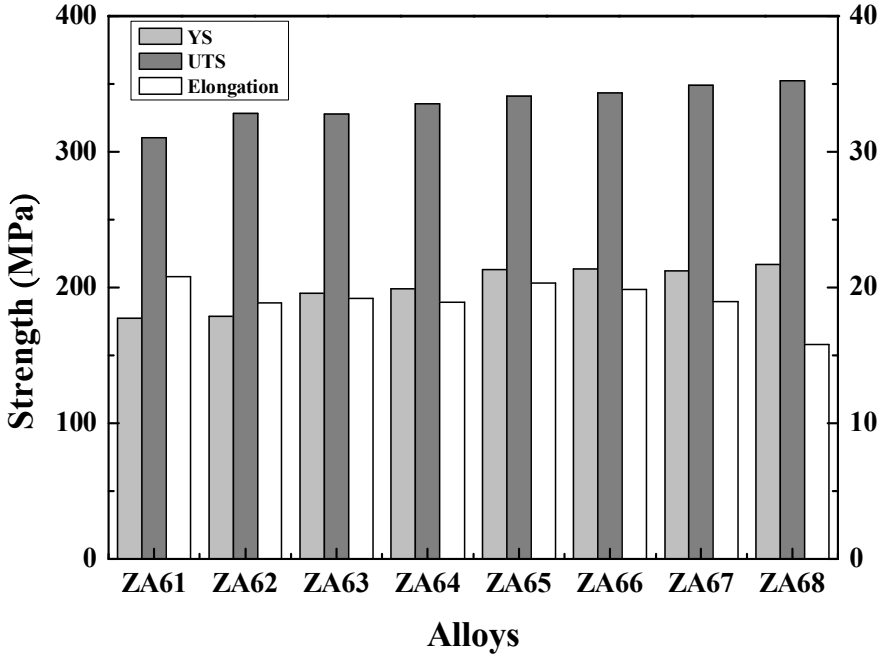

Figure 3.2.14 U.T.S, Y.S. and elongation on tensile test of ZA61-ZA68 alloys extruded at 340^{o}C.

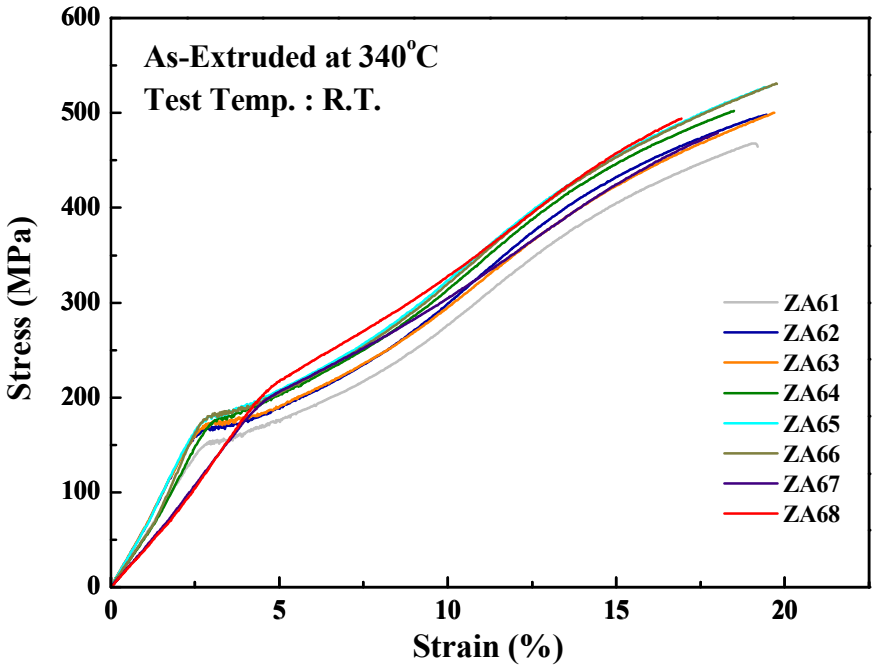

Figure 3.2.15 Compression stress-strain curves of ZA61-ZA68 alloys extruded at 340°C.

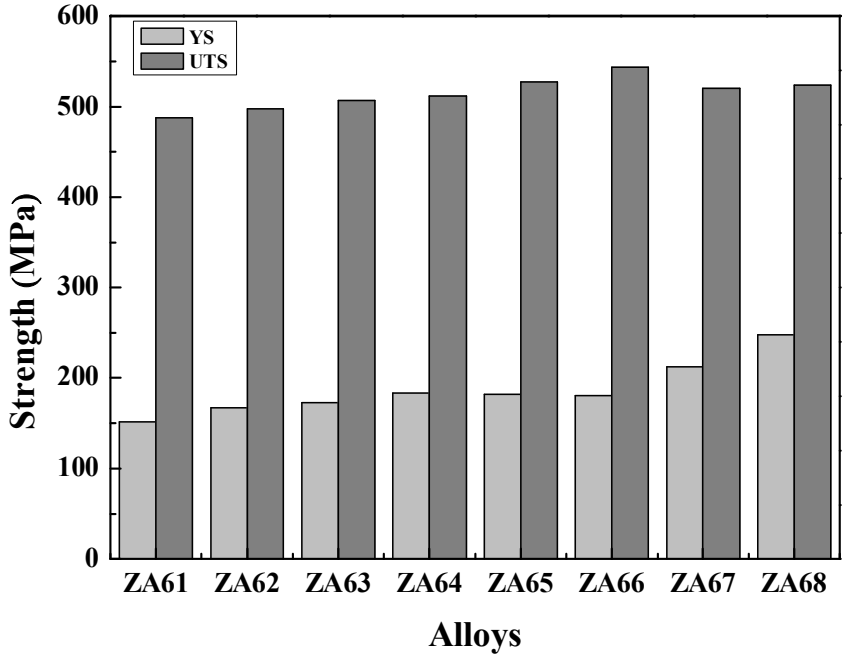

Figure 3.2.16 U.T.S and Y.S. on compression of ZA61-ZA68 alloys extruded at 340^{o}C.

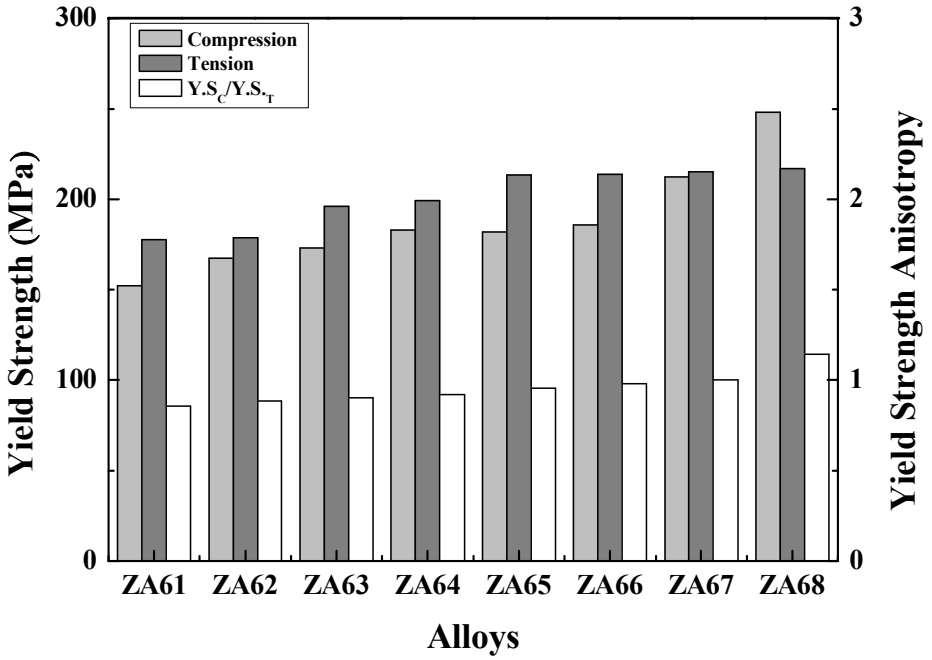

Figure 3.2.17 Yield Strength Anisotropy of ZA61-ZA68 Alloys Extruded at 340^{o}C.

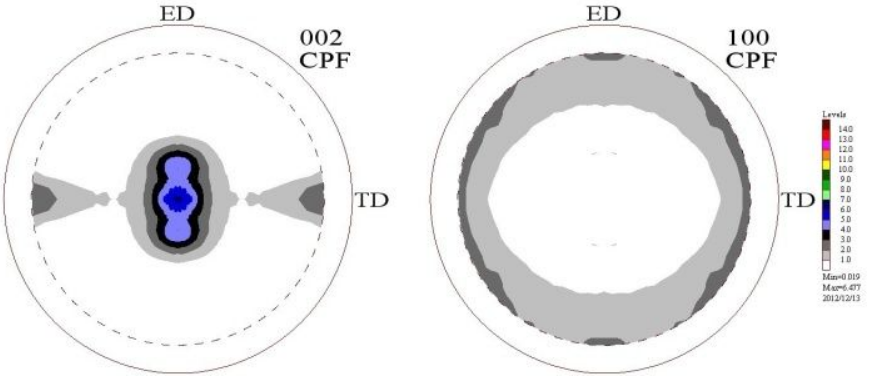

(a)

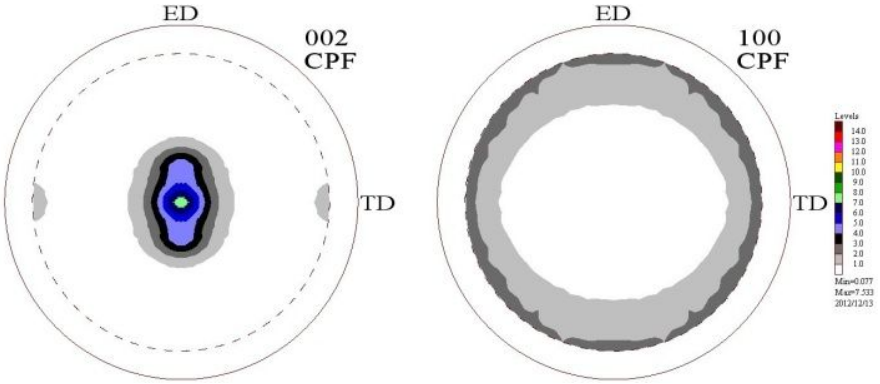

(b)

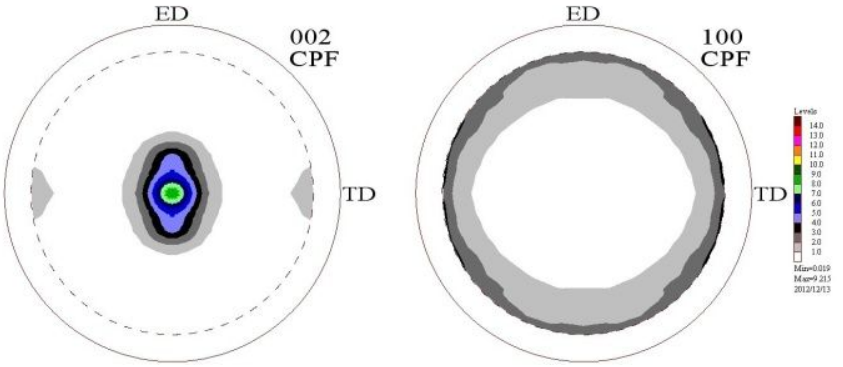

(c)

Figure 3.2.18 Pole figures of ZA alloys extruded at 340°C;

(a) ZA61, (b) ZA64, (c) ZA68alloy

3.2.4 Mechanical properties of ZA71-ZA78 alloys extruded at 340°C.

Figure 3.2.19 ~ Figure 3.2.22 show that the tensile and compressive properties of Mg-7Zn-y (y=1~8) alloys extruded at 340°C. Due to the solid solution strengthening and grain refinement with addition of Al, if the Al increase, the U.T.S. and Y.S. were increased. The compressive stress-strain curves of ZA71-ZA78 showed sigmoidal curves. From the results, the tensile and compressive behavior is similar to the commercial wrought magnesium alloys having basal texture and the mechanical properties of those alloys were increased with addition of Al to the ZA71 alloys due to the solid solution strengthening and grain refinement.

In Figure 3.2.23, the yield strength anisotropy of as-extruded ZA71-ZA78 are plotted. The results show that in the case of the ZA71-ZA78 alloys, the yield strength anisotropy of those alloys is close to 1.0. This means that the difference of yield strength in compression and tension of extrusions is decreased. As mentioned above, yield strength anisotropy is caused by activated tension twin and also in the case of magnesium alloys having very fined grains, twinning is hardly activated in the plastic deformation of magnesium alloys [32, 33].

In order to understand the effect of Zn and Al content on the deformation behavior, the textures of the ZA alloys were examined in the as-extruded condition. The textures of the as-extruded ZA alloys are illustrated in Figure 3.2.24 with the pole figures. It was found that most of the basal poles were parallel to the normal direction, with a slight tendency to incline toward the extrusion direction.

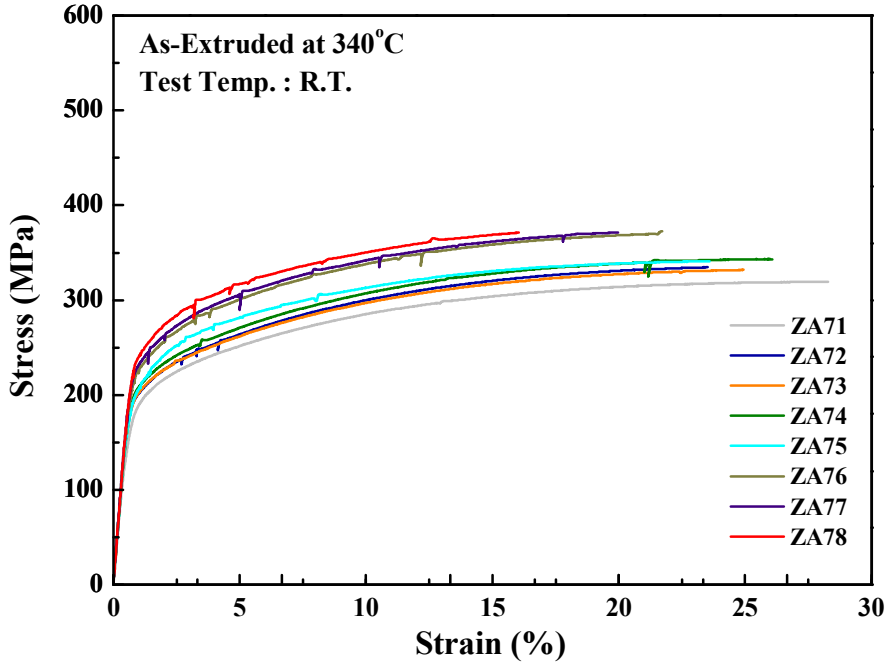

Figure 3.2.19 Tensile stress-strain curves of ZA71-ZA78 alloys extruded at 340°C.

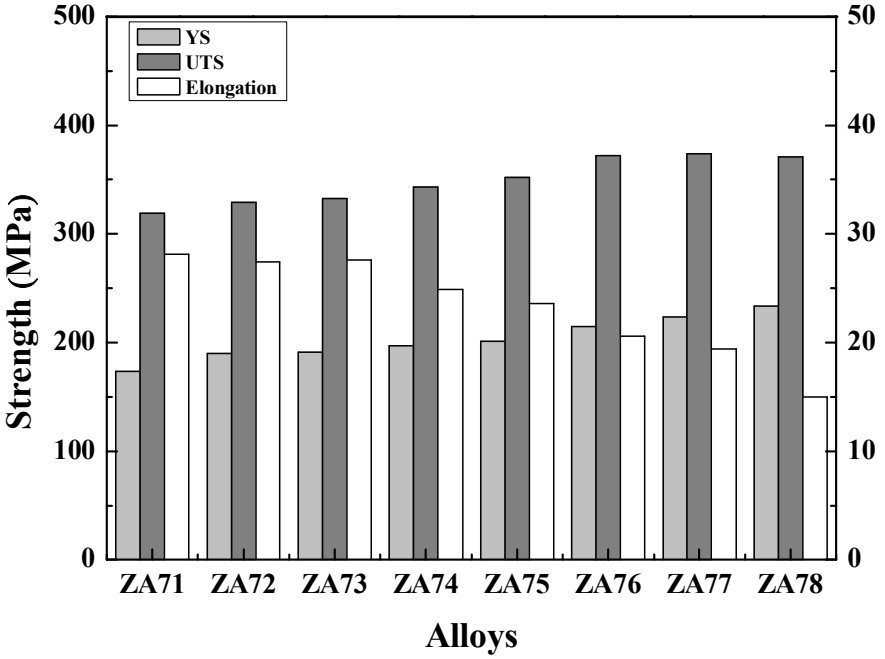

Figure 3.2.20 U.T.S, Y.S. and elongation on tensile test of ZA71-ZA78 alloys extruded at 340^{o}C.

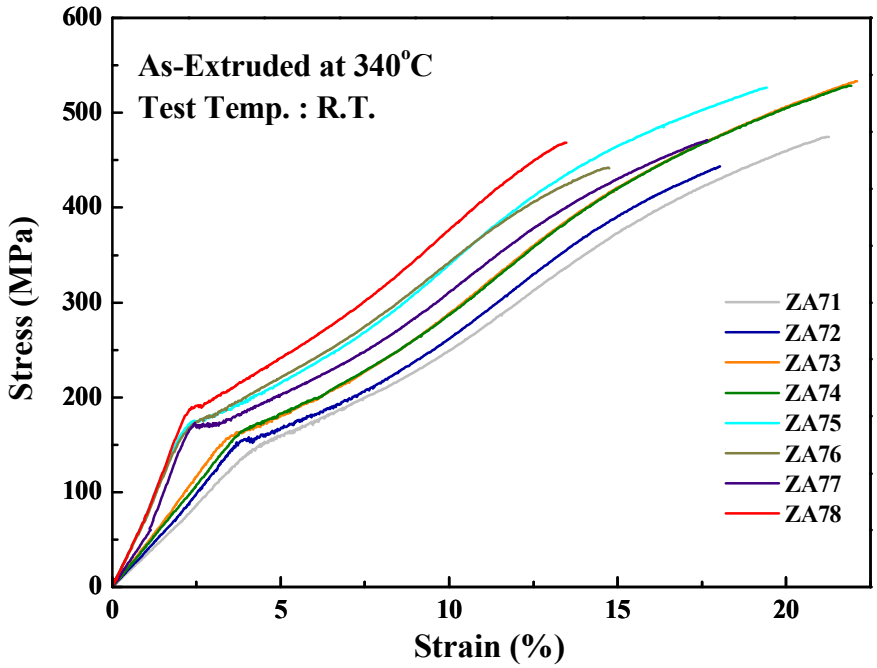

Figure 3.2.21 Compression stress-strain curves of ZA71-ZA78 alloys extruded at 340°C.

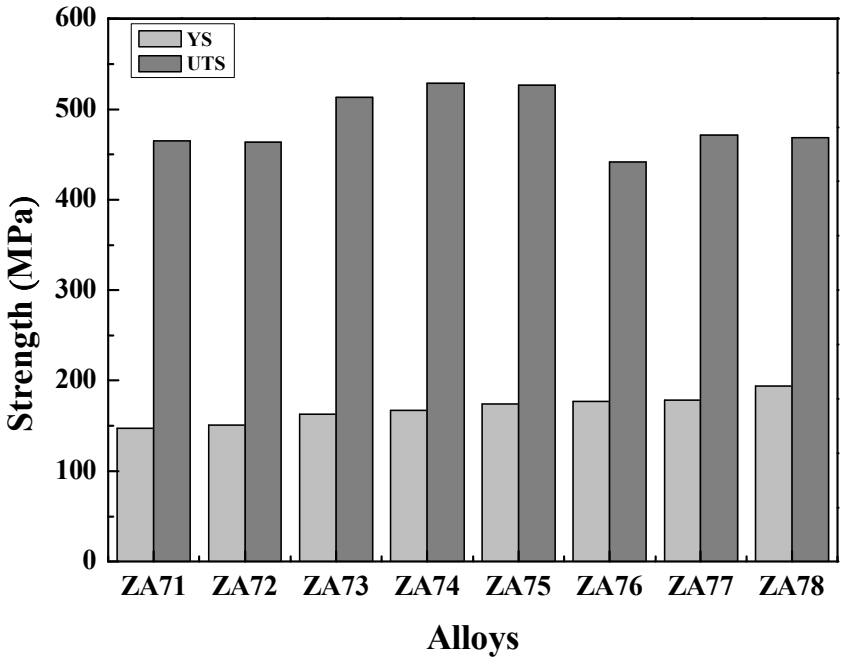

Figure 3.2.22 U.T.S and Y.S. on compression of ZA71-ZA78 alloys extruded at 340^{o}C.

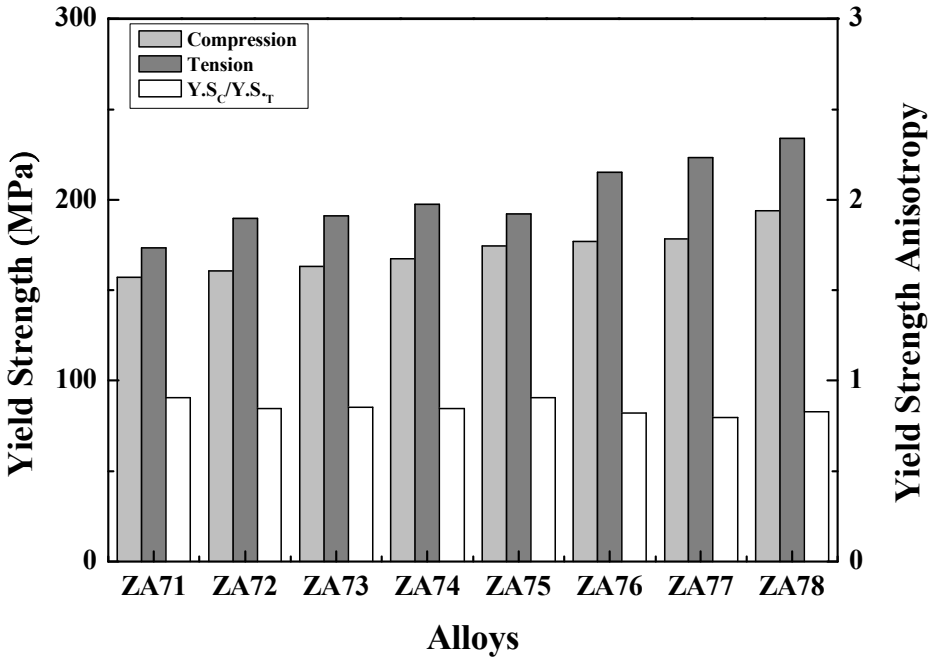

Figure 3.2.23 Yield Strength Anisotropy of ZA71-ZA78 Alloys Extruded at 340^{o}C.

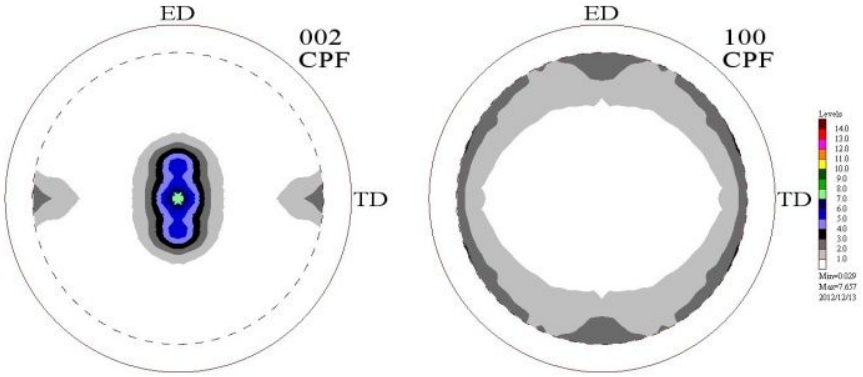

(a)

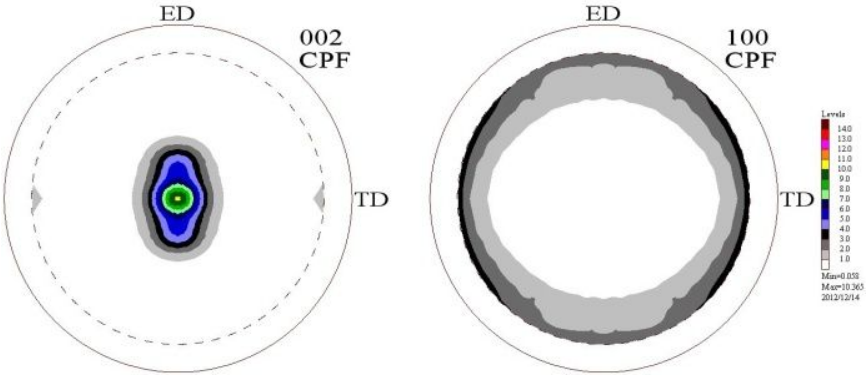

(b)

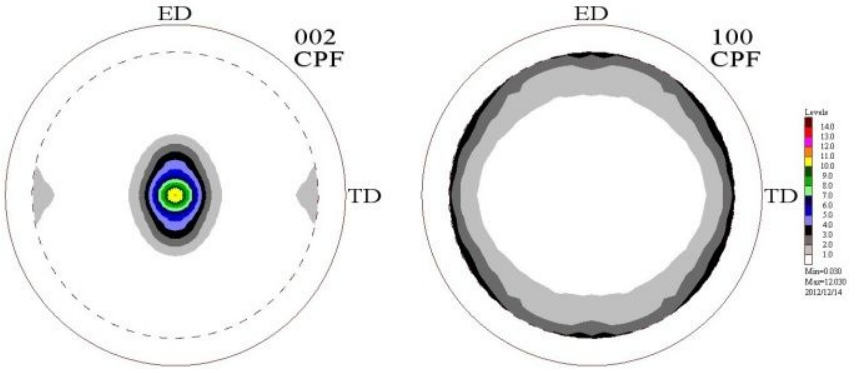

(c)

Figure 3.2.24 Pole figures of ZA alloys extruded at 340^{o}C;

(a) ZA71, (b) ZA74, (c) ZA78 alloy

3.2.5 Mechanical properties of ZA81-ZA88 alloys extruded at 340°C.

Figure 3.2.25 ~ Figure 3.2.28 show that the tensile and compressive properties of Mg-8Zn-y (y=1~8) alloys extruded at 340°C. When the 1 wt.%Zn was added to the ZA81 alloy, the U.T.S. and Y.S. were increased by the solid solution strengthening and grain refinement with addition of Zn. Like general, it is expected that if Al is added to the ZA81 alloy, the mechanical property should be increased by solid solution hardening. The compressive flow curves represented the s-shaped curves that originated from the activation of the tensile twin at an initial stage of compressive deformation.

In Figure 3.2.29, the yield strength anisotropy of as-extruded ZA81-ZA88 are plotted. This means that the difference of yield strength in compression and tension of extrusions is decreased closed to 1.0. Yield strength anisotropy is caused by activated tension twin and also in the case of magnesium alloys having very fined grains, twinning is hardly activated in the plastic deformation of magnesium alloys [32, 33].

In order to understand the effect of Zn and Al content on the deformation behavior, the textures of the ZA alloys were examined in the as-extruded condition. The textures of the as-extruded ZA alloys are illustrated in Figure 3.2.30 with the pole figures. The (0002) planes were found to be nearly parallel to the normal plane of the extruded plates which showed the general characteristics of the extrusion texture of Mg alloys, but the (0002) poles were slightly split into the extrusion directions.

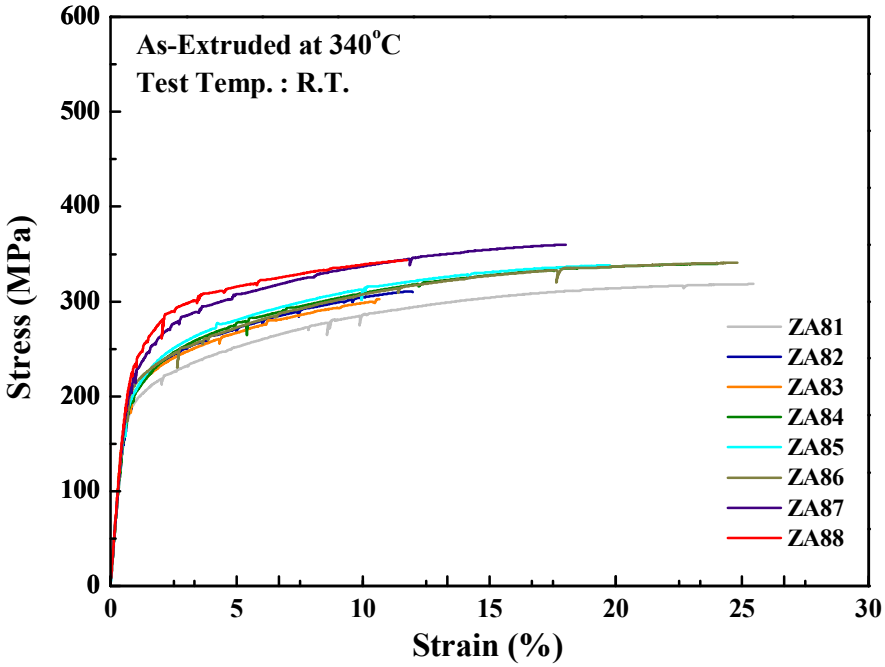

Figure 3.2.25 Tensile stress-strain curves of ZA81-ZA88 alloys extruded at 340°C.

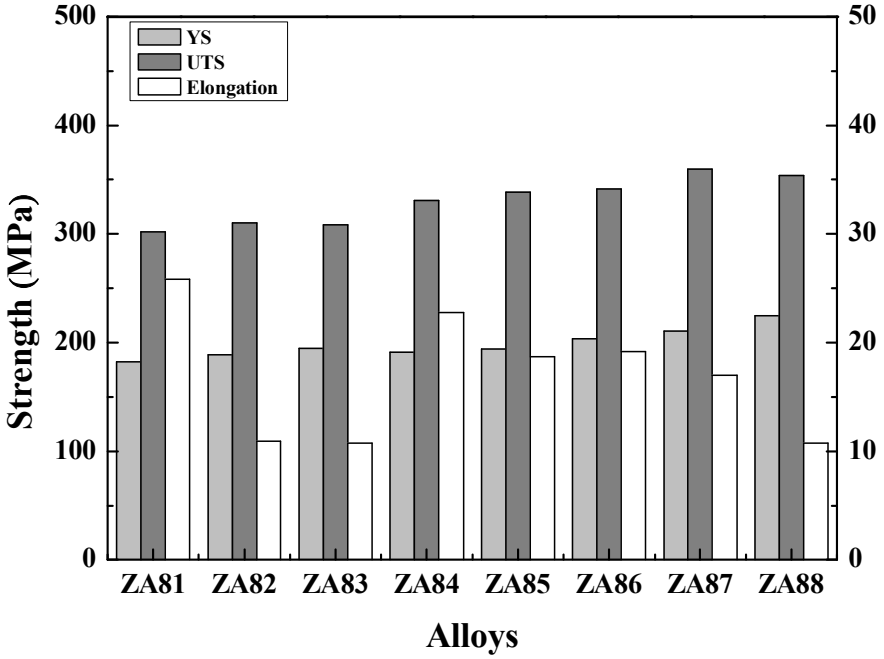

Figure 3.2.26 U.T.S, Y.S. and elongation on tensile test of ZA81-ZA88 alloys extruded at 340^{o}C.

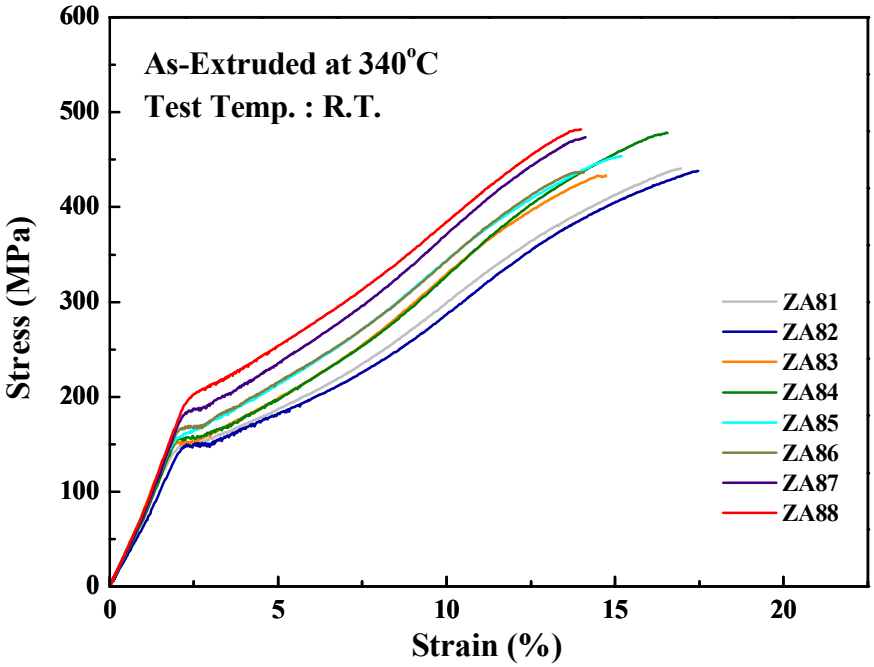

Figure 3.2.27 Compression stress-strain curves of ZA81-ZA88 alloys extruded at 340°C.

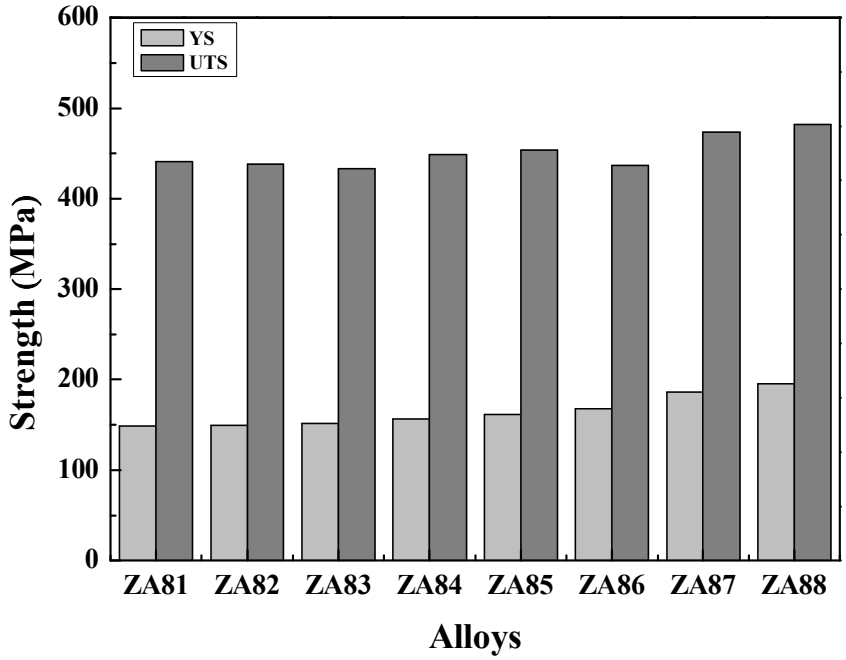

Figure 3.2.28 U.T.S and Y.S. on compression of ZA81-ZA88 alloys extruded at 340^{o}C.

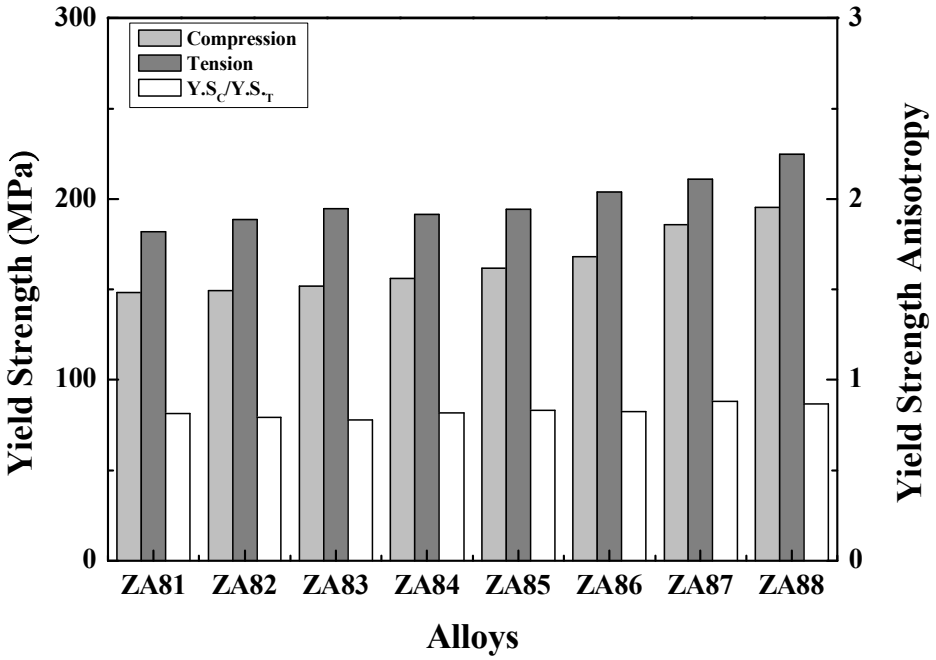

Figure 3.2.29 Yield Strength Anisotropy of ZA81-ZA88 Alloys Extruded at 340^{o}C.

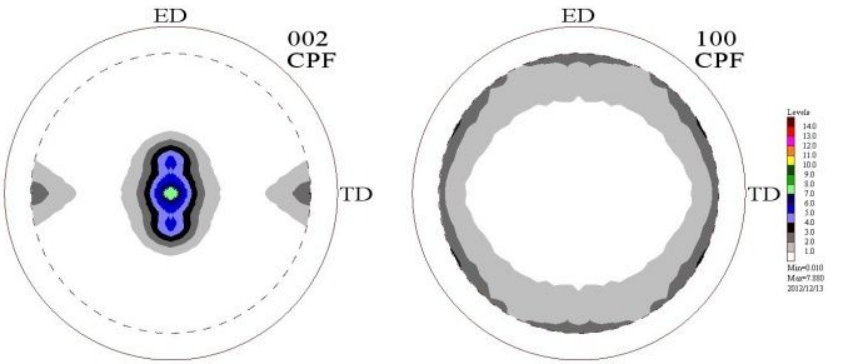

(a)

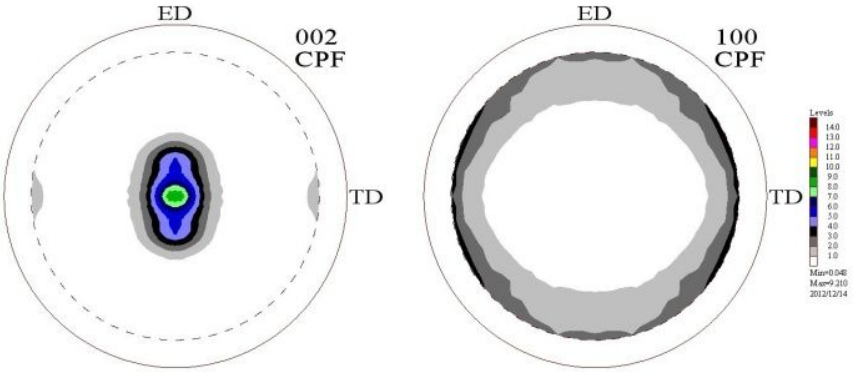

(b)

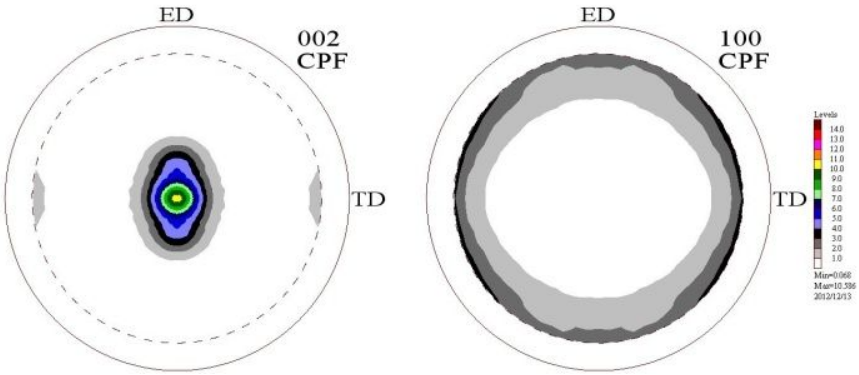

(c)

Figure 3.2.30 Pole figures of ZA alloys extruded at 340^{o}C;

(a) ZA81, (b) ZA84 and (c) ZA88 alloy

4. CONCLUSION

1) The effects of Zn & Al on microstructure extruded at 340 ^{o}C, is that with increasing Zn & Al contents, the grain size is decreasing.

2) In the texture, there is an inclination of basal pole to ND with increasing Zn & Al.

3) With inclination of basal pole to ND, the elongation increase.

4) The maximum intensity of basal pole increase with Zn & Al increasing.

5) With increasing Zn & Al, the elongation decrease and the Y.S. increase.

5. REFERENCES

1. M.Avedesian and H.Baker, "ASM Specialty Handbook: Magnesium and Magnesium Alloys", ASM Int. (1999), pp, 258-263.
2. D.Y.Maeng, T.S.Kim, J.H.Lee, S.J.Hong, S.K.Seo and B.S.Chun, "Microstructure and Strength of Rapidly Solidified and Extruded Mg-Zn Alloys", Scripta Mater, 43 (2000), pp. 385-389.
3. Alan A. Luo. "Materials Comparison and Potential Applications of Magnesium in Automobiles." Magnesium Technology 2000, TMS, pp. 89-98.
4. J.B Clark, "Transmission Electron Microscopy Study of Age Hardening in a Mg-5 wt.% Zn Alloy", Acta Metall., 13 (1965), pp. 1281-1289.
5. I. J. Polmear, "Light Alloys, Metallurgy of the Light Metals", Edward Arnold Ltd. (1995) , pp.218-233.
6. D.Hull and D.J.Bacon, "Introduction to Dislocations", Butterworth-Heinemann, 4th Edition(2001),pp.102-105.
7. Z.Drozd, Z.Trojanova and S.Kudela, "Deformation Behaviour of Mg-Li-Al Alloys", J. of Alloys and Comp., 378(1-2) (2004) , pp. 192-195.
8. A. Luo and M. O. Pekguleryuz, J. Mater. Sci. 29, 5259 (1994).
9. G. S. Foerster, in Proceedings of the IMA 33rd Annual Meeting, Montreal, Quebec, Canada, 23–25 May 1976, p. 35 (1976).
10. W. K. Miller, Metall. Trans. A. 22A, 873 (1991).
11. C. Suman, SAE Internat. Congress and Exposition, Detroit, MI, 25 Feb.-1 March 1991, Paper No. 910416 (1991).
12. M. Ohno, R. Schmid-Fetzer, Z. Metallkd. 96 (2005) 857.
13. E. F. Emley, Principles of Magnesium Technology, p. 969, Pergamon Press, London (1966).
14. I. J. Polmear, "Magnesium Alloys and Applications", Materials Science and Technology, Jan 1994, vol. 10, pp. 1-16.,11.

15. G.V. Raynor. The Physical Metallurgy of Magnesium and its Alloys. New York: Pergamon Press, 1959.
16. M.M. Avedesian, H. Baker, Eds., Magnesium & Magnesium Alloys, ASM International, 1999.
17. A.K. Dahle, Y.C. Lee, M.D. Nave, P.L. Schaffer, and D.H. StJohn, "Development of the As –Cast Microstructure in Magnesium-Aluminum Alloys", Journal of Light Metals, 2001, pp. 61-72.
18. H.E.Friedrich and B.L.Mordike, "Magnesium Technology", Springer (2006), pp. 300-301.
19. H.E. Friedrich, B.L. Mordike Magnesium Technology (Metallurgy, Design Data,Applications) Springer, Berlin (2006).
20. S.R.Agnew, P.Mehrotra, T.M.Lillo, G.M. Stoica and P.K.Liaw, "Texture Evolution of Five Wrought Magnesium Alloys during Route A Equal Channel Angular Extrusion: Experiments and Simulations", Acta Mater., 53 (11) (2005), pp.3135-3146.
21. S.R.Agnew, P.Mehrotra, T.M.Lillo, G.M.Stoica and P.K.Liwa, "Crystallographic Texture Evolution of Three Wrought Magnesium Alloys during Equal Channel Angular Extrusion", Mater. Sci. Eng. A, 408 (1-2) (2005), pp. 72-78.
22. T.Liu, S.D. Wu, S.X. Li and P.J.Li, "Microstructure Evolution of Mg-14% Li-1% Al Alloy during the Process of Equel Channel Angular Pressing", Mater, Scie. Eng. A, 460-461 (2007), pp. 499-503.
23. A.Ma, J.Jiang, N.Saito, I. Shigematsu, Y. Yuan, D. Yang and Y.Nishida, "Imprving both Strength and ductility of a Mg Alloy through a Large Number of ECAP Passes", Mater. Sci. Eng. A, 513-514 (2009), pp. 122-127.
24. H. Watanabe, T. Mukai and K. Ishikawa, "Effect of Temperature of Differential Speed Rolling on Room Temperature Mechanical Properites and Texture in an AZ31 Magnesium Alloy", J. of Mater. Proc. Tech., 182 (1-3) (2007). pp. 644-647.
25. B. Beausir, S. Biswas, D.I.Kim, L.S. Toth and S.Suwas, "Analysis of Microstructure

and Texture Eevolution in Pure Magnesium during Symmetric and Asymmetric Rolling", Acta Mater., 57 (17) (2009), pp.5061-5077.

26. X. Huang, K.Suzuki, A. Watazu, I. Shigematsu and N. Saito, "Effects of Thickness Reduction Per Pass on Microstructure and Texture of Mg-3Al-1Zn Alloy Sheet Processed by Diffenetial Speed Rolling", Scripta mater., 60 (11) (2009), pp. 964-967.
27. ASM Handbook Committee, Alloy Phase Diagrams, ASM International, 1992.
28. Okamoto H, Massalski TB. J Phase Equilibria 1993;14(3):316e35.
29. A. Nayeb-Hashemi and J.B. Clark, The Mg-Mn (Magnesium-Manganese) System, Bull. Alloy Phase Diagrams, 1985, 6(3), p 238-244.
30. Y.C. Lee, A.K. Dahle, and D.H. StJohn, "Grain Refinement of Magnesium", Magnesium Technology, 2000, TMS, pp. 211-218.
31. SOMEKAWA H, SINGH A, MUKAI T. Microstructure evolution of Mg-Zn binary alloy during a direct extrusion process [J]. Scripta Materialia, 2009, 60: 411-414.
32. J. Koike, T. Kobayashi, T. Mukai, H. Watanabe, M. Suzuki, K. Maruyama and K. Higashi, "The Activity of Non-basal Slip Systems and Dynamic Recovery at Room Temperature in Fine-grained AZ31B Magnesium Alloys", Acta Mater., 51 (7) (2003), pp. 2055-2065.
33. Y. Chino, K. Kimura, M. Hakamada and M. Mabuchi, "Mechanical Anisotropy due to Twinning in an Extruded AZ31 Mg Alloy", Mater. Sci. Eng. A, 485 (1-2) (2008), pp. 311-317.